Articles in PresS. J Neurophysiol (January 28, 2004). 10.1152/jn.01121.2003

Intracortical pathways determine breadth of subthreshold frequency receptive fields in primary auditory cortex

Simranjit Kaur, Ronit Lazar and Raju Metherate

Department of Neurobiology and Behavior

University of California, Irvine

Irvine, CA 92697

Running title: Intracortical pathways determine receptive field breadth

Correspondence:

Raju Metherate, Ph.D.

Department of Neurobiology and Behavior

University of California, Irvine

2205 McGaugh Hall

Irvine, CA 92697-4550

phone: (949) 824-6141

fax: (949) 824-2447

e-mail: rmethera@uci.edu

Abstract

To examine the basis of frequency receptive fields in auditory cortex (ACx), we have recorded intracellular (whole-cell) and extracellular (local field potential, LFP) responses to tones in anesthetized rats. Frequency receptive fields derived from excitatory postsynaptic potentials (EPSPs) and LFPs from the same location resembled each other in terms of characteristic frequency (CF) and breadth of tuning, suggesting that LFPs reflect local synaptic (including subthreshold) activity. Subthreshold EPSP and LFP receptive fields were remarkably broad, often spanning five octaves (the maximum tested) at moderate intensities (40-50 dB above threshold). To identify receptive field features that are generated intracortically, we microinjected the $GABA_A$ receptor agonist muscimol (0.2-5.1 mM, 1-5 µl) into ACx. Muscimol dramatically reduced LFP amplitude and reduced receptive field bandwidth, implicating intracortical contributions to these features, but had lesser effects on CF response threshold or onset latency, suggesting minimal loss of thalamocortical input. Reversal of muscimol's inhibition preferentially at the recording site by diffusion from the recording pipette of the $GABA_A$ receptor antagonist picrotoxin (0.01-100 µM) disinhibited responses to CF stimuli more than responses to spectrally distant, nonCF stimuli. We propose that thalamocortical and intracortical pathways preferentially contribute to responses evoked by CF and nonCF stimuli, respectively, and that intracortical projections linking frequency representations determine the breadth of receptive fields in primary ACx. Broad, subthreshold receptive fields may distinguish ACx from subcortical auditory relay nuclei, promote integrated responses to spectrotemporally complex stimuli, and provide a substrate for plasticity of cortical receptive fields and maps.

Introduction

Prominent physiological features of primary ACx include short latency neural responses to CF stimuli, narrow frequency receptive fields (reflected in narrow threshold-tuning functions and response areas), and a topographic arrangement of CF representations (Doron et al. 2002; Merzenich et al. 1975; Phillips et al. 1985b; Sally and Kelly 1988). Similar features are found throughout the lemniscal auditory system (Calford et al. 1983), including in the ventral division of the medial geniculate thalamus (MGv) that provides the the main auditory input to primary ACx (Roger and Arnault 1989; Romanski and LeDoux 1993). Since MGv neurons project to cortical neurons with the same CF (Imig and Morel 1984; Miller et al. 2001; Winer et al. 1999), it is plausible that response characteristics exhibited by cortical neurons simply reflect response characteristics of the afferent thalamic neurons. Similarly, it might seem unlikely that response features in ACx that resemble those seen throughout the lemniscal auditory pathway would reflect a cortical specialization.

Breadth of tuning may be a notable exception. Frequency receptive fields typically are determined using extracellular recordings of spike discharge in response to pure tone stimuli. However, the narrow receptive fields thus derived may be misleading, and underestimate the spectral breadth of inputs to cortical neurons, as evidenced by a number of studies. Blockade of intracortical inhibition results in an expansion of frequency receptive fields derived from extracellular spike discharge, suggesting the presence of normally subthreshold EPSPs that are inhibited by intracortical circuits (Foeller et al. 2001; Muller and Scheich 1988; Wang et al. 2000; Wang et al. 2002). Also, direct, intracellular recordings of synaptic inputs reveal that subthreshold receptive fields extend beyond the boundaries of suprathreshold (derived from

spikes) receptive fields (Ojima and Murakami 2002; Ribaupierre et al. 1972; Volkov and Galazjuk 1991; Wehr and Zador 2003). Subthreshold receptive fields (sometimes referred to as subliminal, surround, or nonclassical receptive fields) could contribute to ACx function in a variety of ways. For example, EPSPs that are subthreshold when evoked by pure tones could integrate, spatially and temporally, with other EPSPs elicited by spectrotemporally complex stimuli to elicit spikes. Further, in aroused or attentive animals, or animals undergoing behavioral training with acoustic stimuli, receptive fields could be larger, or differently shaped, than those observed under anesthesia (Edeline et al. 2001; Weinberger and Bakin 1998). Finally, changes in synaptic strength of previously subthreshold inputs by behavioral (or other) manipulations could underlie large scale reorganization of frequency representations in ACx (Kilgard and Merzenich 1998; Recanzone et al. 1993).

The present study was designed to answer two questions central to the issue of subthreshold receptive fields in ACx: i) how broad are they, and ii) to what extent do they involve integration of thalamocortical and intracortical inputs? We made intracellular and LFP recordings of tone-evoked responses to measure synaptic activity, focusing on the initial, presumed excitatory, components. We determined onset latencies for responses to CF and nonCF stimuli, to infer functional connectivity from the arrival time of acoustic inputs. We then determined the effect of intracortical muscimol microinjections on receptive field bandwidth, since this manipulation should preferentially inhibit cortical (vs. thalamocortical) neurons. And finally, we reversed the effect of intracortical muscimol preferentially at the recording site (within a larger, muscimol-inhibited cortical region) to distinguish between two hypotheses of the functional connectivity underlying receptive fields. The results indicate that, at a given cortical site, thalamocortical and intracortical pathways preferentially mediate responses to CF and nonCF stimuli, respectively.

Materials and Methods

Surgical procedure

All procedures were in accordance with the NIH guide for the Care and Use of Laboratory Animals and approved by the University of California, Irvine IACUC. Male Sprague-Dawley rats (Charles River Laboratories, Hollister, CA), age >1 month and weighing 110-240 g were used for combined intracellular and LFP studies. Adult rats weighing 250-500 g were used for LFP-only studies. Animals were anesthetized with 1.5 g/kg urethane i.p. (Sigma, St. Louis, MO) and 10 mg/kg xylazine i.p. (Phoenix Pharmaceuticals, St. Joseph, MO) and subsequently administered 0.6 mg/kg atropine i.p. (Phoenix). Animals remained in a state of deep anesthesia throughout the surgery and were given supplemental injections of urethane (40 mg) and xylazine (0.25 mg) at ~2 h intervals to maintain areflexia and a synchronized cortical EEG. Body temperature was maintained at 36-37 ^{o}C using a feedback-controlled heating pad (Harvard Instruments, Holliston MA). The animal was placed in a sound-attenuating chamber (model AC-3, IAC, Bronx NY) mounted on an air table (Newport, Irvine CA), and the head was secured in a stereotaxic frame (model 923, Kopf Instruments, Tujunga CA) using blunt earbars (Kopf). A midline incision was made and xylocaine ointment (AstraUSA, Westborough, MA) was applied to the incision. After the skull was cleared, the head was secured by a custom-made head holder screwed and cemented onto the skull. A craniotomy was performed over the right ACx and the exposed cortex was kept moist with warmed saline. The earbars were removed. In early experiments, a drawing of the surface vasculature helped with reconstruction of recording sites. In most experiments, a Polaroid picture was taken of the exposed cortex through the surgical

microscope (Carl Zeiss, Thornwood NY) for the same purpose. To improve stability during experiments that included intracellular recordings, tracheal cannulation, lumbar suspension and drainage of the cisterna magna were performed in addition to the surgery described above. These procedures helped minimize brain pulsations caused by blood pressure fluctuations and respiration. After the experiments animals were euthanized with a lethal dose of anesthesia.

Electrophysiology

Primary ACx in the rat lies on the dorsolateral aspect of temporal cortex, framed by a characteristic blood vessel pattern (Sally and Kelly 1988). Recording from the cortical surface within this area, we used short-latency, large amplitude responses to click stimuli to localize ACx (Barth and Di 1990; Shaw 1988), and then made multiple penetrations into layer 4 of the cortex to confirm the tonotopic arrangement characteristic of primary ACx (Doron et al. 2002; Horikawa et al. 1988; Kilgard and Merzenich 1998; Sally and Kelly 1988).

Intracellular recording. Methods for *in vivo* whole-cell recordings are similar to those described previously (Metherate and Ashe 1993a). Patch pipettes were pulled from glass (1.5 mm o.d. glass, A-M Systems, Carlsborg WA) on a horizontal puller (P-97, Sutter Instruments, Novato CA) and had a tip diameter of approximately 2.5 μm and resistances ranging from 8-14 MΩ when filled with (in mM): K^+-gluconate, 140; MgCl, 1; CaCl, 1; HEPES, 10 and EGTA, 1.6; adjusted to pH 7.3 with KOH. The osmolality of the recording solution was adjusted to about 260 mmol/kg. All drugs and chemicals were obtained from Fisher (Fair Lawn NJ), with the exception of D-gluconic acid which was obtained from Sigma Chemical Co. (St. Louis MO).

Whole-cell recordings were made from neurons in layers 2-4 as described previously (Blanton et al. 1989; Metherate and Ashe 1993a). Briefly, the electrode was inserted

perpendicular to the pial surface, lowered to a depth of ~200 μm using a microdrive (Inchworm, Burleigh Instruments, Fishers NY) and weak positive pressure applied to avoid clogging the electrode tip (positive or negative pressure was applied through the side-port of the sealed electrode holder (Warner Instruments, Hamden CT). The positive pressure was then removed and the electrode was advanced slowly, with a current pulse (100 pA, 30 ms) delivered once per second. Proximity to a neuron's membrane produced an increased voltage response to the current pulse, at which time the application of a small amount of negative pressure resulted, ideally, in an increased voltage response that eventually indicated a tight seal (~1 GΩ). When a stable gigaohm seal was achieved, steadily increasing negative pressure was applied to rupture the membrane. Occasionally, the membrane ruptured spontaneously. A successful rupture was indicated by the sudden appearance on the oscilloscope of a membrane potential (approximately -70 mV) with rhythmic voltage fluctuations (Metherate and Ashe 1993a).

Responses to acoustic stimuli were recorded using an intracellular amplifier (Axoclamp 2B, Axon Instruments, Foster City CA), viewed on a digital oscilloscope (Tektronix, Irvine CA), digitized at 5 kHz (IT-16, Instrutech, Port Washington NY), averaged (20 or 40 trials) and stored on a computer (Macintosh G4, Apple Computer). Data acquisition was triggered 100 ms before acoustic stimulation. Computer software (AxoGraph, Axon Instruments) controlled data acquisition and analysis.

Extracellular recording. LFP recordings were obtained in nearly all experiments using glass microelectrodes (1.5 mm o.d. glass, A-M Systems; tip diameter ~2.5 μm, filled with 1 M NaCl, ~1 MΩ impedance at 1 kHz) pulled in multiple stages to obtain blunt tips, as for patch pipettes. In two experiments, dual tungsten electrodes were used for simultaneous recording from two sites (1-2 mm separation). Electrodes were inserted perpendicular to the pial surface, and

movement was controlled using a microdrive (Burleigh Inchworm). Neural activity was filtered and amplified (1 Hz-10 kHz, AI-401 CyberAmp, Axon Instruments) displayed on the oscilloscope, digitized at 5 kHz and stored on computer. Data acquisition was triggered 100 ms before acoustic stimulation, and responses were averaged (25 or 50 trials; AxoGraph, Axon Instruments). The local EEG was monitored continuously on the oscilloscope.

Acoustic stimulation

Pure tone stimuli were digitally synthesized and controlled using MALab (Kaiser Instruments, Irvine CA) and a dedicated computer (Macintosh PowerPC, Apple Computer) and delivered through an electrostatic speaker (ES-1 with ED-1 driver, Tucker-Davis Technologies, Gainesville, FL) positioned ~3 cm in front of the left ear. For calibration (SPL in decibels re: 20 µPa) a microphone (model 4939 microphone and Nexus amplifier; Bruel and Kjaer, Norcross GA) was positioned in place of the animal at the tip of the left earbar. Tones were 100 ms in duration with 10 ms linear rise and fall ramps.

Pharmacological manipulations

To inhibit intracortical activity, muscimol hydrobromide (5.1 mM in saline; Sigma) was administered through a glass micropipette with a broken tip (~20-30 µm diameter) attached via polyethylene tubing to a 1 or 5 µl Hamilton syringe (WPI, Sarasota FL). The pipette was inserted into the cortex at the recording site after removal of the recording electrode. Muscimol (or saline, for controls) was injected in increments of 0.5-1.0 µl over 1-2 min, or, in one early experiment, muscimol was applied to the cortical surface. The muscimol pipette was left in place for 15 min after the injection, and then removed and replaced with the recording electrode, after which tone-

evoked responses were obtained. In some cases, this procedure was repeated one or more times to increase the muscimol dose. In later experiments, to investigate reversal of inhibition by picrotoxin (0.01-100 μM in saline; Sigma), we used a lower concentration of muscimol (200 μM, 0.5-2.0 μl). After recording responses in muscimol-inhibited cortex, the recording electrode was replaced with one containing picrotoxin.

Analysis of acoustic-evoked responses

CF and other acoustic response features were determined for a particular recording site by examining LFPs evoked by a standard stimulus set of six frequencies spanning five octaves (1 or 1.25 kHz to 40 kHz in ~one octave steps) delivered at intensities from 70 dB SPL to below CF threshold, typically in 10 dB steps. Although the one-octave resolution of the stimulus set is relatively crude, it was sufficient to determine changes in tonotopic organization over the cortical distances examined (~1 mm steps), and we use the conventional term "CF" for convenience. CF was determined qualitatively by identifying the frequency of the stimulus with the lowest threshold response. When stimuli of more than one frequency elicited a response at threshold, intensity was varied by 5 dB and/or CF was determined by the response with the shortest onset latency (e.g., Fig. 3A, responses at 0 dB). Quantitative measures of evoked intracellular and LFP onset latencies (see details below) and peak amplitudes were obtained for all responses. For measurements of response amplitude, baseline was defined as the average potential from tone onset to 5 ms after stimulus onset.

We defined a “response” at each recording site as a voltage deflection exceeding two standard deviations from the mean baseline obtained from all responses to the standard stimulus set (typically 48 responses: 6 frequencies x 8 intensities). Two additional criteria were helpful

near threshold: a voltage greater than two standard deviations was considered a response only when i) there were clear responses to the same frequency stimulus at higher intensities, and ii) the onset latency was equal to or greater than the latency at higher intensities.

A major part of the present study involved obtaining objective and accurate estimates of response onset latencies. The method is illustrated in Fig. 2B for an LFP. First, a "threshold" one standard error below the mean baseline was established, and the point at which the response crossed the threshold determined. Then, two points 1 ms before and after the threshold-crossing were identified, and the slope of the line connecting these two points was determined. Finally, the intersection of this line with the average baseline potential was obtained and defined as response onset (Fig. 2B, small arrow). A similar procedure was used to obtain the onset latencies of intracellular responses.

Statistical analyses

Statistical analyses were performed using Statview (v. 4.5 for Macintosh, Abacus Concepts). Tests on independent means were Student's t-test and factorial ANOVA, whereas the paired t-test and Repeated Measures ANOVA were used for related means. In analyzing response features obtained at different frequencies and intensities (e.g., Fig. 3C), Repeated Measures ANOVAs were performed separately at each intensity; for such ANOVAs only a subset of the data were included so that the mean values being compared contained equal 'n' (however, all data are plotted in figures). Detailed statistics results are in the figure legends; $p < 0.05$ was considered significant.

Results

We have investigated the functional connectivity underlying frequency receptive fields in primary ACx by recording tone-evoked, synaptic responses (intracellular recordings) and presumed synaptic responses (LFPs) in 50 rats. The data comprise intracellular and LFP responses to a standard set of six frequencies (1 or 1.25, 2 or 2.5, 5, 10, 20 and 40 kHz) spanning five octaves at up to nine stimulus intensities. We also employed pharmacological manipulations designed to distinguish between thalamocortical and long-distance, intracortical connectivity. Although the latter portions of the study utilize only LFP recordings, we first describe intracellular synaptic responses to acoustic stimuli obtained in whole-cell recordings, and compare them to LFP recordings obtained at the same location to confirm that LFP characteristics reflect those of known synaptic responses.

Intracellular recordings in primary ACx

We obtained intracellular recordings from 8 neurons in primary ACx, using the *in vivo* whole-cell recording method (Metherate and Ashe 1993a). Cell depths ranged from 275 to 612 μm below the pia, corresponding to layers 2-4. In cell-attached mode, the seal resistance was 1.0 ± 0.1 GΩ; following rupture of the membrane with suction, the resting membrane potential (RMP) was –69 ± 3.2 mV and the input resistance, estimated from responses to small hyperpolarizing current pulses, was 182 ± 64.2 MΩ. The duration of recording ranged from 9 to 47 min.

Example intracellular responses to acoustic stimulation are shown in Fig. 1A (top traces), for a layer 3 neuron. For this neuron, rupture of the cell membrane was obtained using minimal suction after the seal resistance had reached a plateau at 1.5 GΩ. Following break-in, rhythmic membrane potential fluctuations characterized spontaneous activity as described previously (Metherate and Ashe 1993a; Metherate et al. 1992). The RMP was –81 mV immediately upon break-in, but generally ranged from –52 to –63 mV for most of the recording (RMP defined as the potential during the peak hyperpolarizing phase of membrane potential fluctuations, in the absence of injected current). Spontaneous action potentials occurred during depolarizing phases of membrane potential fluctuations in about half the neurons. In most neurons, we made small adjustments in the level of injected DC current over time to maintain the membrane potential close to the RMP observed at the beginning of each data collection sequence. However, data obtained when the RMP was more depolarized than –50 mV were discarded.

Figure 1

Figure 1A (top traces) shows synaptic responses to the standard set of six frequencies at 20 dB and 70 dB SPL. At the lower intensity, only 10 kHz stimuli produced a clear, short latency depolarization; i.e., 10 kHz was CF. At the high intensity, stimuli of all frequencies elicited EPSPs, followed by apparent IPSPs which were more clearly visible at the edges of the receptive field (e.g., responses to 1.25 kHz and 40 kHz in Fig. 1A). Note that in other neurons IPSPs were not always visible at RMP as overt hyperpolarizations, nor were they restricted to the receptive field edges. Also apparent in the figure is that EPSP onset latencies decreased with increasing stimulus intensity, and increased with increasing spectral distance from CF (see also Fig. 2A, C).

The receptive field bandwidth derived from tone-evoked EPSPs was broad, measuring at least 5 octaves (the maximum we could test) at 70dB for the example in Fig. 1A. Across neurons, bandwidth ranged from 3 to ≥5 octaves at moderate to high intensities (Fig. 1B). At 10 and 20 dB above threshold, where determination of bandwidth was not limited by the 5 octave stimulus range, EPSP bandwidth averaged 1.25 ± 0.75 octaves and 2.75 ± 0.85 octaves, respectively (Fig. 1C). Although stimuli were delivered in relatively crude, one octave steps, these bandwidth estimates indicate remarkably broad synaptic receptive fields.

Tone-evoked EPSPs typically did not elicit spikes unless the neuron was depolarized with DC current, but in three neurons, higher-intensity stimuli did elicit spikes at RMP. Stimuli up to one octave above CF (n = 2) or two octaves below CF (n = 1) produced suprathreshold responses, and spike-based bandwidth ranged from 1-2 octaves. In contrast, subthreshold bandwidth in these cells ranged from 3 to ≥5 octaves. In other words, subthreshold receptive fields were much broader than spike-based receptive fields.

Comparing intracellular and LFP responses to pure tones

After each intracellular recording, LFPs were recorded at the same location to allow for a direct comparison of intracellular and LFP features (n = 7). LFPs were recorded using electrodes similar to patch pipettes, but with slightly larger tips and correspondingly lower impedances (~1 MΩ). Fig. 1A (bottom traces) shows an LFP recording from the same layer 3 site as the intracellular responses (top traces). Tone-evoked LFPs were invariably of negative polarity, as expected for extracellular responses near the site of excitatory synaptic activity (Barth and Di 1990; Metherate and Ashe 1993b; Metherate et al. 1992; Muller-Preuss and Mitzdorf 1984). As can be seen in Fig. 1A, several LFP features resemble those of intracellular responses: both sets

of responses indicate a CF of 10 kHz (sole, or shortest-latency, response at 20 dB), a bandwidth ≥ 5 octaves at 70 dB, and similar changes in onset latency with increasing intensity or spectal distance from CF (also see Fig. 2A).

Group data confirm the similarities between intracellular and LFP responses. CFs derived from intracellular and LFP responses were identical in 5/6 cases (in one cell, the intracellular CF could not be determined clearly). However, CF thresholds were higher in intracellular recordings (average 40 ± 5.5 dB, range 20-50 dB) compared to LFP recordings (average 30 ± 5.5 dB, range 10-40 dB; paired t-test, $n = 5$, $p < 0.001$). Bandwidths for paired intracellular and LFP recordings are shown in Fig 1B, and covered a similar range at each intensity up to the maximum detectable 5 octaves at high intensities. At 10 dB and 20 dB above threshold, where bandwidth determination was not limited by our stimulus range, intracellular and LFP bandwidth did not differ (Fig. 1C).

An important goal of this study was to infer functional connectivity, in part from differences in onset latency among LFP responses to stimuli of different frequencies. We therefore examined EPSP and LFP onset latencies, and found that the response to CF stimuli had the shortest onset latency while the responses to nonCF stimuli—both higher and lower frequencies—were progressively longer with increasing spectral "distance" from CF. An example is shown in Fig. 2A, using intracellular and LFP recordings from the same site. For LFPs (Fig. 2A, top traces) and EPSPs (bottom traces), CF (10 kHz) stimuli elicited the shortest onset latency and responses to stimuli of other frequencies tended to have progressively longer latency onsets with increasing spectral distance from CF. Note that this trend holds for frequencies above and below CF; e.g., LFP and EPSP responses to stimulus frequencies two octaves above and below CF (40 kHz and 2.5 kHz, respectively), all have longer latency onsets than do responses to stimuli at CF.

Figure 2

As can be seen for some traces in Fig. 2A, the exact timing of individual onsets was not always clear, especially when the onset was not abrupt. The difficulty in identifying onset precisely led us to devise an objective method for estimating onset latency. The method is illustrated in Fig. 2B for an LFP response, and is detailed in the Methods. Briefly, onset latency was determined by extrapolating a line based on the slope of the LFP around a threshold point established from statistical variations (-1 SE) in the baseline potential. A threshold relatively near to the baseline was chosen because response onset often seemed to begin well before the strongest portion of the response, producing an initially gradual, two-component onset (Fig. 2B). A near-baseline threshold ensured that the early component of the response influenced our estimate of onset latency, and resulted in more accurate estimates than if the strongest portion of the response was extrapolated to the baseline instead. Average LFP latencies are described in greater detail below (Fig. 3C), and clearly show increasing onset latencies with spectral distance from CF.

Intracellular onset latencies were determined similarly. Onset latency data at 70 dB (~20-30 dB above threshold) showed that CF stimuli tended to have the shortest onset latency (average 18.5 ± 1.53 ms, range 12.9-26.8 ms) with responses to nonCF stimuli having progressively longer onset latencies with distance from CF. However, a wide range of response latencies resulted in limited statistical significance (Fig. 2C).

Taken together, the comparison of intracellular and LFP data in terms of polarity, bandwidth, and changes in onset latency with intensity and spectal distance from CF, demonstrate that LFPs

reflect important features of local synaptic activity. Since LFPs are suitable for the long duration recordings needed for this study, at a pre-determined depth (layer 4) in each animal, and before and after pharmacological manipulations, we subsequently focused on LFPs to infer synaptic connectivity in ACx.

Layer 4 LFP response to pure tones

In 25 animals, we recorded tone-evoked LFP activity in multiple penetrations across ACx. These multiple penetrations were performed to confirm the topographic arrangement of frequency representations expected for primary ACx, and to determine which, if any, features of LFP responses varied across frequency representations (changes in response features observed in multiple penetrations across ACx also would support further the notion that LFPs reflect local activity). At each site, the recording depth was kept constant at 600 µm to sample activity in layer 4 (in five experiments, current source density analysis revealed the major short-latency, tone-evoked current sink to be at 600 µm; data not shown). To determine CF and other response features, we used the same standard, five-octave stimulus set as before. In each animal we first determined the area responsive to sound stimuli by recording surface responses to clicks. We made a first penetration near the anterior end of the shortest-latency, largest amplitude surface responses (click map), and recorded layer 4 responses to the stimulus set. We then made 1-4 additional penetrations in ~1 mm steps directly posterior to the first penetration, and recorded layer 4 responses to the same stimulus set. In most animals (n = 19) we observed a shift in effective stimuli from high frequencies at the anterior penetration to lower frequencies at more posterior locations (arrows in Fig. 3 and subsequent figures indicate CF threshold). This

sequence is consistent with previous reports of the tonotopic organization of primary ACx in the rat (Doron et al. 2002; Horikawa et al. 1988; Sally and Kelly 1988).

Figure 3

In the 19 animals with a confirmed tonotopic arrangement, the region of the first penetration was invariably a high frequency area with CF = 40 kHz (Fig. 3B). Since 40 kHz was the highest frequency delivered, these anterior sites might actually have higher CFs. However, the threshold intensity at these sites was relatively low, averaging 9.5 ± 1.6 dB SPL (range 0-20 dB SPL), similar to thresholds seen in more posterior penetrations with lower frequency CFs (below). Thus, the anterior sites likely have CFs near 40 kHz. In each animal with a tonotopic arrangement, responses revealed a lower-frequency region at a second site more posterior to the "high-frequency site" (Fig. 3A, B). This "mid-frequency site" was 1.5-2 mm posterior (mean 1.7 ± 0.1 mm). CF at the mid-frequency site was usually 10 kHz (n = 15), but sometimes 5 kHz (n = 3) or 20 kHz (n = 1). Thresholds at the mid-frequency sites averaged 16.3 ± 3.3 dB SPL (range 0-40 dB SPL), not different from those at the high-frequency site (paired t-test, n = 19, $p > 0.05$).

In 6/25 animals examined for frequency organization, no clear evidence for tonotopy emerged. In these animals, 2-4 penetrations were made spanning a distance of 0.8-2.8 mm (mean 1.7 ± 0.3 mm) from the anterior portion of the click map, i.e., the same procedure that revealed tonotopy in most animals. Unlike in the animals with clear tonotopy, however, several sites up to 2.8 mm apart appeared to have the same CF (n = 5), and/or some sites responded weakly at threshold to a range of frequencies spanning three octaves or more (n = 2). For the latter animals, small and variable responses near threshold prevented a clear determination of CF, and therefore

may have prevented determination of a progression of CFs with distance. However, CFs were clear in other cases that did not show a change of CF with distance. Further, responses at higher intensities were robust in all six animals, yet 5/6 did not show the expected shift of frequency ranges with distance (cf. responses at 30 dB SPL in Figs. 3A and 3B for expected shift). The surface blood vessel patterns and distribution of click responses in these animals appeared similar to tonotopic animals, suggesting that recordings were made in analogous cortical regions. However, absent a fine-grain mapping procedure it remains possible that we were recording in a non-primary field (Doron et al. 2002; Horikawa et al. 1988; Sally and Kelly 1988). In any case, data from animals lacking tonotopic organization were not analyzed further.

Features of tone-evoked responses that imply connectivity

For the 19 animals with confirmed recordings in tonotopic primary ACx, we undertook a detailed analysis of the layer 4 responses to the standard stimulus set. For each animal, data were analyzed both at the high-frequency site (CF = 40 kHz) and at the mid frequency site (CF generally 10 kHz). We first analyzed the onset latency of tone-evoked LFP responses, since minimum onset latencies at a particular site are determined, in part, by anatomical connections. As is clear from the LFP examples already described (Figs. 2A, 3A, 3B), and from the mean LFP onset latencies in Fig. 3C, onset latency increased for stimulus frequencies away from CF at both high- and mid-frequency sites. Changes in onset latency were smaller, yet still significant, at higher intensities; e.g., for the mid-frequency site in Fig. 3C, changes in onset averaged 4.3 ms/octave at 10 dB and 0.7 ms/octave at 60 dB above threshold (data averaged in one octave intervals from –3 to +1 octaves from CF). Onset latencies for CF stimuli decreased with increasing intensity at each site (Fig. 3C, ANOVAs, p values < 0.01), and appeared to asymptote

at higher intensities (50-60 dB, Fig. 3D). Finally, for a given intensity, CF stimulus-evoked onset latencies at the high-frequency site were consistently less than those at the mid-frequency site (Fig. 3D).

Note, as previously mentioned (Fig. 1), that LFP responses at moderate to high intensities could span five octaves. Even more remarkably, such data at a high-frequency site indicate a receptive field extending at least five octaves *below* CF (for an individual example, see Fig. 4C). These broad receptive fields are similar to the subthreshold receptive fields seen in intracellular recordings (Fig. 1) but substantially broader than those derived from suprathreshold (single unit) activity in primary ACx (see Discussion).

Measurements of LFP peak amplitude (Fig. 2B) often showed the expected decreased amplitudes at stimulus frequencies away from CF (e.g., Fig 3A, B). However, a more striking—and unexpected—feature observed in many animals was an *increased* amplitude for stimulus frequencies below CF, especially at high intensities (Fig. 4). Examples of this "boosting" of response amplitudes to below-CF stimuli are shown in Figs. 4A and C (boosting defined as response amplitudes to nonCF stimuli greater than amplitudes to CF stimuli). Prominent boosting occurred in 19/38 sites in 14/19 animals, and always at frequencies below CF (Fig. 4E). Boosting also occurred in intracellular recordings, in 2/8 cells, at high intensity (Fig. 4D). Note in the example (Fig. 4A, C) and the mean data (Fig. 4E) that boosting is seen for stimuli up to 3 octaves below CF at both mid- and high-frequency sites. Note, also, that despite the boosting of responses to nonCF stimuli, the response to CF stimuli still had the shortest onset latency (Fig. 4B; peak amplitudes normalized to facilitate comparison of onsets). Intracellular recordings confirmed shorter onset latencies for CF stimulus-evoked EPSPs despite boosting of responses to nonCF stimuli (Fig. 4D). The effects of boosting dominated the average data at higher

intensities for stimulus frequencies below CF (Fig. 4E). Response amplitudes to CF stimuli increased monotonically, on average, with increasing stimulus intensity, even when analyzing data only from sites displaying boosted responses.

Figure 4

Two hypotheses on the connectivity underlying frequency receptive fields

LFP features have important implications for how frequency receptive fields are constructed in ACx. For example, at a given recording site, CF stimuli elicit the shortest latency responses, implying a direct anatomical connection from the thalamus. NonCF stimuli—up to five octaves from CF—elicit longer latency responses. Two hypotheses posit extreme scenarios to account for how CF and nonCF information arrive at a given recording site (Fig. 5; for this exercise, we loosely define "nonCF"as several octaves from CF). In the first (Fig. 5A), extensive thalamocortical terminal arbors project over a wide cortical area and thus relay nonCF as well as CF information to the recording site. According to this scheme, increased latencies for nonCF input could result from longer thalamocortical path lengths. In the second scenario (Fig. 5B), nonCF information arrives at the recording site via an intracortical mono- or poly-synaptic pathway. The increased latency for nonCF input therefore results from intracortical processing that includes one or more synaptic delays. (An additional factor, that nonCF stimuli elicit longer latency spikes than CF stimuli throughout the auditory system, applies to both hypotheses but does not account for the small timing differences among synaptic onsets observed here; see Discussion). The remainder of this study is aimed at distinguishing between these two hypotheses.

Figure 5

Inhibition of intracortical activity via muscimol microinjection into ACx

To examine the involvement of intracortical processing in relaying CF vs. nonCF inputs, we inhibited intracortical activity with microinjections of muscimol, a $GABA_A$ receptor agonist that inhibits postsynaptic activity but not fiber activity (for review, see Martin and Ghez 1999).

In nine experiments, after recording baseline responses we applied muscimol (5.1 mM; 1–2.5 µl) to the mid-frequency recording site. In four of these nine experiments muscimol was microinjected (1.0 µl) into layer 4. In one experiment muscimol was applied to the cortical surface. In another four experiments we made 2-5 injections into layer 4, typically 0.5 µl per injection, 30-60 min apart with intervening recordings that revealed progressively stronger suppression, and we assumed cumulative doses because the effects of muscimol at this concentration are long lasting (present study, Edeline et al. 2002; Martin and Ghez 1999). Muscimol at such doses would be expected to diffuse several millimeters from the injection site (Edeline et al. 2002; Martin and Ghez 1999) and inhibit much of primary ACx. We began data collection ~15-20 min after the muscimol injection(s). Muscimol strongly reduced CF stimulus-evoked LFP magnitude for hours (Fig. 6A; recovery was attempted in one case, with ~50% recovery seen after 6 h). On average, muscimol significantly reduced response peak amplitude for intensities at and above threshold (Fig. 6B), and reduced completely the later components of evoked responses (Fig. 6A). In 6/9 animals, threshold either did not change (Fig. 6A, arrowhead indicates pre-drug CF threshold) or increased 10 dB. In 3/9 animals, threshold after muscimol increased 20 to 40 dB. Nonetheless, muscimol did not significantly change average CF threshold

(2.2 ± 2.22 dB before muscimol vs. 13.3 ± 4.71 dB after; paired t-test, n = 9 pairs, p = 0.062). As a control for nonspecific effects, injection of 0.5 µl (n = 1 animal) or 1 µl (n = 4) saline at the recording site did not affect responses to CF stimuli (93.1 ± 6.2% of pre-drug amplitude, all intensities pooled; Fig. 6B), whereas 1 µl muscimol reduced amplitudes to 25.7 ± 2.1% of baseline (paired t-test with all intensities pooled, $p < 0.05$). Saline also did not affect response threshold (pre-drug threshold 4.0 ± 2.45 dB vs. 4.0 ± 2.45 dB after saline; paired t-test, n = 5 pairs, $p > 0.05$). Similarly, as can be seen in Fig. 6B, saline did not affect the mean response amplitude at threshold (pre-drug 89.9 ± 17.22 µV vs. 84.7 ± 10.15 µV after saline, paired t-test, n = 5 pairs, $p > 0.05$).

Figure 6

We also analyzed the effect of muscimol on responses to CF stimulus onset. While muscimol appeared to increase onset latency in some cases (e.g., 50 dB response in Fig. 6A), this effect was not consistent. On average, muscimol tended to not alter onset latency (Fig. 6C). The lack of a consistent effect on CF threshold and onset latency suggests that these features depend more on monosynaptic activity—thalamocortical input—than on intracortical processing (see Discussion for full rationale). Conversely, the strong reduction of the response peak amplitude, and the complete reduction of later components of the response, implicates intracortical amplification of thalamocortical input.

The reduction of response magnitude to CF stimuli with no consistent change in onset latency or threshold suggested that muscimol was acting as desired—inhibiting intracortical

activity without affecting thalamocortical input. We therefore examined the effect of muscimol on responses to nonCF stimuli, since preferential reduction of such responses would support the hypothesis that intracortical pathways mediate nonCF inputs (Fig. 5B) whereas equivalent reduction of responses to CF and nonCF stimuli would suggest that intracortical pathways contribute similarly to both (Fig. 5A). An example of muscimol's effect is shown in Fig. 7A. As in the previous example, muscimol reduced responses to CF stimuli but did not change CF threshold (arrow). However, response amplitudes to nonCF stimuli were also reduced, and in many cases, reduced fully. When averaged data were compared for inhibition of responses to CF vs. nonCF stimuli (nonCF data from 1-3 octaves below CF combined), only small differences emerged (Fig. 7B). However, the reduction of responses to nonCF stimuli appeared more prominent at the frequencies most spectrally-distant from CF. Since the complete reduction of these responses necessarily would reduce bandwidth, we quantified bandwidth for individual sites and then determined average bandwidth at each intensity. An analysis of bandwidth 20-70 dB above the threshold for CF stimulus-evoked responses showed that muscimol reduced breadth of tuning 20-50 dB above threshold (Fig. 7C; muscimol had no significant effect 60-70 dB above threshold, but note that our detection limit of 5 octaves probably precluded measurement of full pre-drug bandwidths).

Figure 7

We also examined the effects of intracortical muscimol on boosting. Muscimol reduced boosted responses, but abolished boosting in only 2/8 animals ("boosting" defined as a response to a nonCF stimulus greater than that to a CF stimulus; pre-muscimol boosting occurred in 8/9

animals). An example is seen in Fig. 7A, where pre-muscimol boosting is prominent at 70 dB. Although muscimol strongly reduced all response amplitudes, the response to CF stimuli still appears weaker than the response at –3 octaves (1.25 kHz), i.e., some boosting remained in muscimol (see also group data in Fig. 9A).

The reduction in mean bandwidth by muscimol suggests that breadth of tuning reflects intracortical processes (Fig. 5B). However, it is also possible that the reduction of responses to near-baseline levels could artifactually produce a reduction in bandwidth by preferentially reducing responses to nonCF stimuli below our response threshold (defined as 2 standard deviations from the mean baseline, see Methods). Such an effect on bandwidth might be more prominent at lower intensities, where boosting is not seen and responses to nonCF stimuli are smaller than responses to CF stimuli. To resolve this issue, we designed a final experiment to reverse the muscimol effect preferentially at the recording site, and determined the effects of this manipulation on responses to CF and nonCF stimuli.

Local reversal of inhibition at the recording site after inhibition of ACx by muscimol

In this final experiment, we added picrotoxin (a $GABA_A$ receptor channel blocker) to the recording electrode after recording responses in muscimol-inhibited ACx (Fig. 8A). Our rationale was the following: if thalamocortical pathways preferentially mediate responses to CF stimuli and intracortical pathways preferentially mediate responses to nonCF stimuli (Fig. 5B), then reversing muscimol's inhibition *only at the recording site* should preferentially restore responses to CF stimuli. If, on the other hand, thalamocortical inputs contribute equally to CF and nonCF stimulus–evoked responses (Fig. 5A), then reversing muscimol's effect at the recording site should restore responses to CF and nonCF stimuli equally. We therefore

determined the effects of local picrotoxin application on intensity functions (LFP amplitude vs. stimulus level) for CF (10 kHz) and nonCF (1.25 kHz) stimuli, using a nonCF stimulus three octaves below CF to minimize the possibility that picrotoxin could diffuse to the main cortical representation of the nonCF stimulus.

Figure 8

In preliminary experiments, we found that even high concentrations of picrotoxin were ineffective in reversing the effects of 5.1 mM muscimol, despite the noncompetitive nature of picrotoxin's block. After experimenting with lower doses of muscimol, we determined that 200 μM muscimol could be antagonized successfully. In 8 animals we first recorded intensity functions at CF and nonCF before and after microinjections of muscimol (3-5 μl of 200 μM). We then placed an electrode containing picrotoxin (0.01-100 μM) at the recording site and obtained tone-evoked responses, alternating between CF and nonCF stimuli. An example is shown in Fig. 8B, and averaged data are shown in Fig. 9A. The lower concentration of muscimol effectively reduced response amplitudes, and picrotoxin partially reversed the inhibited responses. However, picrotoxin produced greater recovery of responses to CF stimuli than to nonCF stimuli (Figs. 8B, 9). As a control for nonspecific effects, in 2 animals injection of 3 μl saline at the recording site did not affect responses to CF stimuli (95.6 ± 12.5% of baseline amplitude), whereas 3 μl muscimol reduced amplitudes to 37.8 ± 7.2% of baseline (paired t-test with pooled responses to 40-60 dB stimuli, $p < 0.05$), and the addition of pictrotoxin to the recording electrode reversed the inhibition (87.9 ± 16.3% of control, paired t-test vs. saline, $p > 0.05$).

The averaged data in Fig. $9A_i$ show that muscimol markedly reduced response amplitude to CF stimuli and picrotoxin produced partial recovery that approached control amplitudes at high intensities. The average data in Fig. $9A_{ii}$ show that muscimol also reduced response amplitudes to nonCF stimuli but that reversal by picrotoxin was weaker. In Fig. 9B, plotting the muscimol and picrotoxin data relative to pre-drug amplitudes reveals more clearly the greater reversal of suppression for response amplitudes to CF vs. nonCF stimuli. Note that the picrotoxin effect varied with intensity (CF data in Fig. 9B). These data support the idea that CF information is relayed directly to the recording site by thalamocortical projections, whereas nonCF input arrives preferentially via intracortical pathways (Fig. 5B).

Figure 9

Discussion

We have used whole-cell intracellular and LFP recordings to investigate how frequency receptive fields within primary ACx are generated. Intracellular recordings revealed that subthreshold receptive fields are substantially broader than suprathreshold (derived from spikes) receptive fields described in this and earlier studies. Receptive fields were equally broad in intracellular and LFP recordings. Cortical microinjection of the $GABA_A$ receptor agonist muscimol reduced the bandwidth of LFP-based receptive fields in layer 4, indicating that intracortical pathways contribute to broad receptive fields. Delivery of the $GABA_A$ antagonist picrotoxin to the recording site after widespread muscimol-induced inhibition preferentially

disinhibited responses to CF stimuli over responses to nonCF stimuli. These data suggest that intracortical integration underlies broad frequency receptive fields in primary ACx.

Intracellular and LFP responses to tones: do LFPs reflect local EPSPs?

In the present study, the principal response features common to whole-cell and LFP recordings from the same site included: i) similar CFs, ii) similar breadth of frequency receptive fields at each intensity tested, iii) receptive field breadth ≥5 octaves at moderate to high intensities, and iv) minimum response latencies to CF stimuli and progressively longer onset latencies to stimuli with increasing spectral distance from CF. The main differences between intracellular and LFP responses were that intracellular recordings tended to have higher thresholds at CF and longer latencies than corresponding LFPs. These data indicate that LFPs reflect synaptic potentials in a local group of neurons with similarly broad spectral integration centered on the same CF, but with varied thresholds and onset latencies (LFP latencies and thresholds likely reflect those of neurons with the shortest latencies and lowest thresholds).

LFPs are considered an extracellular reflection of synchronous synaptic potentials and are especially clear in laminated structures such as hippocampus and neocortex (Eggermont and Smith 1995; Johnston and Wu 1995). Data from simultaneous extracellular and intracellular recordings in ACx *in vitro* and *in vivo* have demonstrated that electrical stimulation of afferents at intensities that consistently produce subthreshold EPSPs invariably elicits LFPs and synaptic potentials of opposite polarity but with similar latencies (Cruikshank et al. 2002; Hsieh et al. 2000; Metherate and Ashe 1994, 1993b; Metherate and Cruikshank 1999). In particular, in the auditory thalamocortical slice preparation, MG stimulation evokes layer 4 EPSPs and LFPs with virtually identical onset latencies (Cruikshank et al. 2002). Thus, LFPs can be useful for

exploring synaptic connectivity, as in the present study. While the exact volume over which LFP activity can be detected is unknown, note that CFs differed between recording sites separated by 1 mm or less. Such differences might not exist if neural activity from distant frequency representations could be detected by the recording electrode, and suggest that high-impedance LFP electrodes sample activity over a distance ≤1 mm. Although measures of single unit activity are more precise in terms of localizing neural activity and bear a clearer neural basis, advantages of LFPs include the measurement of presumed subthreshold activity (e.g., can be used to determine breadth of total synaptic input) at predetermined recording sites (e.g., layer 4), and recordings that are reproducible and stable (Barth and Di 1990; Eggermont 1996; Galvan et al. 2001; Norena and Eggermont 2002; Ohl et al. 2000; Steinschneider et al. 1999). Conversely, despite the advantages of LFPs the uncertainty about the volume over which summed neural activity is recorded requires intracellular confirmation of critical features.

Functional connectivity inferred from response to CF stimuli

At a given recording site CF stimuli evoked the shortest onset latency, which was expected given previous observations of minimum spike latency at CF (Brugge et al. 1969; Eggermont 1996; Phillips and Hall 1992). However, CF stimuli at the high frequency site evoked shorter latency onsets than did CF stimuli at the mid frequency site (average 1.5 ms difference). Shorter minimum spike latencies for higher-frequency CF stimuli have been observed throughout the auditory system, including cochlear nerve (Evans 1972; Kiang 1965), cochlear nucleus (Kitzes et al. 1978), inferior colliculus (Langner et al. 1987; Sanes and Constantine-Paton 1985), and auditory cortex (Mendelson et al. 1997; but see Phillips 1998a), and likely result from timing differences in the transduction of acoustic stimuli in the cochlea; i.e., high frequency stimuli are

transduced near the base of the basilar membrane whereas low-frequency stimuli are transduced further along the basilar membrane closer to its apex. Rough estimates of travel time along the basilar membrane based on published accounts of cochlea, cochlear nerve, and cochlear nucleus recordings (Evans 1972; Kiang 1965; Kitzes et al. 1978; Robles and Ruggero 2001) range from 0.3-0.7 ms/octave, similar to the ~0.75 ms/octave obtained in the present study. These findings suggest that precise response timing is maintained throughout the auditory system (Heil and Irvine 1997). Such precision must reflect specialized synaptic mechanisms at each level of the auditory "labeled line" (Oertel 1999; Trussell 1999), and similar specializations may exist in ACx as well (Metherate and Aramakis 1999).

The notion of a labeled line implies that CF input to neurons in primary ACx comes from MGv neurons with the same CF. Supporting evidence is provided by the effects of muscimol in the present study, which imply long-lasting inhibition of cortical neurons with little effect on afferent (thalamocortical) axons (Edeline et al. 2002; Talwar et al. 2001). Whereas muscimol significantly reduced LFP amplitude and receptive field bandwidth, CF stimulus-evoked response threshold and onset latency did not change significantly, suggesting that these features rely on monosynaptic thalamocortical afferents (see next section for detailed rationale). Similarly, the lack of a consistent effect on CF stimulus-evoked response threshold and onset latency suggests that muscimol microinjections into the cortex did not diffuse to the thalamus. These findings are consistent with the results of studies using physiological recordings and anatomical tracing to show that like-CF regions of ACx and MG interconnect (Imig and Morel 1984; Winer et al. 1999). Also, cross-correlated unit recordings of MG and ACx neurons indicate functional connectivity when CFs are within one-third of an octave (Miller et al. 2001).

Thus, thalamocortical afferents convey to cortex information regarding frequencies preferentially at or near CF.

Using muscimol to distinguish thalamocortical from intracortical processes

In theory, inhibition of cortical activity by muscimol does not prevent thalamocortical afferents from releasing transmitter, but the resulting monosynaptic EPSPs would be small amplitude due to sustained shunting of the postsynaptic neuron by open Cl^- channels, and less likely to elicit spikes. The inhibition of postsynaptic spiking would preclude polysynaptic (intracortical) activity. The effect on LFP responses elicited by stimulation of afferents entering the inhibited region would be to reduce amplitudes completely except for the earliest (monosynaptic) portion of the response, which would have an amplitude that was reduced (though not completely) and no change in onset latency. In the present study, muscimol, in the volumes and concentrations used, was expected to diffuse several millimeters from the injection site and produce significant inhibition of neurons over a large portion of primary ACx (Edeline et al. 2002; Martin and Ghez 1999). CF stimulus-evoked LFPs were reduced as would be expected for preferential inhibition of polysynaptic over monosynaptic activity (i.e., without change in onset latency, with partial reduction of early response components, and with complete suppression of later response components). Moreover, the presence of a presumed monosynaptic LFP component, along with the minimal effects of muscimol on response threshold at CF, suggest that muscimol did not diffuse so far as to reach the MG and inhibit thalamocortical relay neurons. Thus, the use of muscimol should help distinguish thalamocortical from intracortical processes.

Since muscimol delivery in the present study involved injection of microliter volumes into ACx, it was necessary to demonstrate that the effects attributed to muscimol did not result from the volume of fluid injected. In addition to the slow rate of injection (0.5-1.0 µl over 1-2 min) and the 15-20 min delay after injection before data collection was begun (to ensure that compression effects dissipated), several results attest to the pharmacological nature of muscimol's actions. First, muscimol reduced neural response amplitude 74% whereas saline injections of the same volume produced only 7% reductions. Second, in one animal, surface bath application of muscimol produced inhibition similar to that produced by intracortical microinjections in other animals. Third, neither muscimol nor saline significantly affected response threshold—presumably a vulnerable response because of its small amplitude—and saline did not affect response amplitude at threshold (6% reduction). Fourth, the inhibitory effects of muscimol were reversed by picrotoxin after sequential injections of saline and muscimol, whereas damage to the cortex would have resulted in progressively smaller responses after each injection. Together, these results demonstrate that the muscimol's effects were largely due to actions at receptors, and not to damage from injected volumes.

In this context, it is not entirely clear why reversal by picrotoxin varied with intensity (Fig. 9B). One possibility is that damage to the recording site from muscimol injections may be more evident at lower intensities, although the lack of significant changes to response threshold after saline or muscimol injections argues against such damage. Alternatively, more intense stimuli may activate greater numbers of neurons and thus may be more likely to include neurons affected by the diffusion of picrotoxin from the recording pipette. In contrast, the few neurons activated at threshold may not include those neurons closest to the recording pipette and the picrotoxin diffusing from it.

Functional connectivity inferred from responses to nonCF stimuli: the basis of broad receptive fields

LFP recordings demonstrated responses to nonCF stimuli up to 5 octaves from CF, with onsets occurring progressively later than the onset of responses to CF stimuli. We consider three hypotheses to explain these data, and their implications for functional connectivity in ACx:

1. NonCF input is carried by the same thalamocortical afferents as CF input, but thalamic neurons spike at longer latencies to nonCF stimuli thus producing longer-latency synaptic onsets in ACx. At all levels of the auditory system neurons spike to nonCF stimuli at longer latencies than to CF stimuli (Brugge et al. 1969; Eggermont 1996; Hind et al. 1963; Kitzes et al. 1978; Phillips and Hall 1992). Thus, a thalamocortical neuron would relay nonCF information at longer latencies, resulting in longer latency synaptic (and LFP) onsets in ACx. This scenario, while undoubtedly correct, does not seem to account for the onset latencies evoked by nonCF stimuli in the present study. Published quantitative examples of single unit responses to CF and nonCF stimuli indicate approximate changes in minimum spike latency of 12-60 ms/octave for ACx (10-30 dB above threshold, data for intervals less than one octave are extrapolated, Brugge et al. 1969; Eggermont 1996; Phillips and Hall 1992), 4-8 ms/octave for inferior colliculus (10 dB above threshold, Hind et al. 1963) and 8-15 ms/octave for cochlear nucleus (50-60 dB above threshold, Kitzes et al. 1978). These latency ranges are generally much longer than the 0.7-4.3 ms/octave for 60-10 dB above threshold in the present study (LFP responses in Fig. 3C). Also, the reduction of bandwidth by intracortical muscimol, and the differential disinhibition of responses to CF stimuli over responses to nonCF stimuli by picrotoxin suggests that nonCF

information is not carried by the same afferents that relay CF information. Together, these observations indicate that even though thalamic neurons may spike to nonCF stimuli at long latencies, those spikes do not mediate the earliest arrival of nonCF input at the cortical recording site.

2. NonCF input is via divergent thalamocortical projections delivering CF input to other sites (Fig. 5A). In this scenario, broadly divergent thalamocortical projections provide CF input to one cortical site and nonCF information to other sites. The divergent terminal arbor could produce slightly longer latencies for responses to nonCF stimuli relative to responses to CF stimuli, i.e., the longer path length of thalamocortical collaterals may increase conduction delay by a few milliseconds. There is insufficient information available about thalamocortical afferents and collaterals to evaluate this idea on the basis of conduction delay. However, the hypothesis is inconsistent with the effects of muscimol and picrotoxin in ACx. Specifically, if responses to nonCF stimuli were produced by monosynaptic thalamocortical input, then muscimol would not affect receptive field bandwidth, and picrotoxin at the recording site would restore responses to CF and nonCF stimuli equally. In contrast, muscimol decreased bandwidth, and picrotoxin had little effect on inhibited responses to stimuli three octaves below CF. These data indicate that bandwidth does not depend on divergent thalamocortical projections.

3. NonCF input to a site is via intracortical projections (Fig. 5B). In this scenario, thalamocortical CF input to a given site is subsequently relayed intracortically to provide nonCF input to other sites. The intracortical relay would account for the nonCF stimulus-evoked response's greater sensitivity to muscimol, lesser sensitivity to picrotoxin, and delayed onset

latency relative to CF stimulus-evoked responses. The delay in onset latency should increase progressively for responses to stimuli both higher and lower than CF since spectral distance from CF would be related monotonically to physical distance between frequency representations in the cortex (Doron et al. 2002; Sally and Kelly 1988). We consider this hypothesis to be the best supported by the data. Further support is provided by preliminary data on tone-evoked current-source-density (CSD) analyses: whereas CF stimulus-evoked current sinks always are found in the middle layers (layers 3 and 4) where thalamocortical inputs terminate (Roger and Arnault 1989; Romanski and LeDoux 1993), nonCF stimulus-evoked sinks lie either above or below the CF stimulus-evoked sink in 6/7 animals (R. Lazar and R. Metherate, unpublished observations). Similarly, the proposed intracortical flow of information has been confirmed using the auditory thalamocortical brain slice preparation (Cruikshank et al. 2002; Rose et al. 2003): electrical stimulation of the MG results in a focused, short latency LFP in layer 4 and longer latency LFPs at more distant cortical sites (also recording within layer 4 but across presumed isofrequency bands). Laminar recordings reveal a current sink in layer 4 at the site of the shortest latency LFP, and current sinks generally outside of layer 4 at the more distant cortical sites. Together, these data suggest that CF information from MGv is relayed through layer 4 to other regions of primary ACx, contributing to the synaptic integration underlying broad receptive fields.

Implications of below-CF "boosting"

Although we expected LFPs evoked by CF stimuli to exhibit greater peak amplitudes than LFPs evoked by other frequencies, this often was not the case. Response boosting occurred at high intensities in most animals, up to three octaves below CF (never at frequencies above CF), and at both mid- and high-frequency sites. Since boosted responses at times were associated

with weak responses to isointensity CF stimuli, it seemed possible that neurons with nonmonotonic rate-level (intensity) functions may contribute to them, i.e., boosted responses might actually reflect reduced responses to CF stimuli rather than enhanced responses to below-CF stimuli. However, LFP intensity functions at CF were monotonic. Also, single unit studies have shown that neurons with nonmonotonic intensity functions have enclosed (circumscribed) response areas (e.g., Phillips et al. 1985b); we find no evidence in the literature that these neurons have enhanced responses to stimulus frequencies below CF. Nonetheless, since the relationship of LFP and unit activity is unclear, it is possible that neurons with nonmonotonic intensity functions may contribute to boosted responses (or, more precisely, to weakened responses to CF stimuli) in the present study. Boosting may help equalize spike latencies to CF and nonCF stimuli for some neurons, or contribute to the propagation of activity from low to high frequency regions observed with optical recording methods (Hess and Scheich 1996); the functional relevance of this activity, however, is unclear. As muscimol reduces, but does not abolish, boosting, it appears to originate subcortically and be amplified in ACx. In fact, auditory nerve fibers with CFs above 1 kHz exhibit responses that qualitatively resemble boosting at higher intensities (Rose et al. 1971), but the effect is weaker than that seen in ACx both in terms of the spectral distance from CF of the boosted response (e.g., < 1 octave) as well as the degree of boosting.

How broad are frequency receptive fields in primary ACx?

Intracellular and LFP receptive field bandwidths measured ≥5 octaves at moderate to high intensities, and averaged 2-3 octaves 20 dB above threshold. At the mid-frequency site, the average LFP bandwidth 20 dB above threshold of 2.4 octaves (Fig. 7C) corresponds to an

approximate bandwidth measure of 2.71 $kHz^{0.5}$ using the square root transformation, and 0.54 using a "Q" measure similar to Q_{10}, but 20 dB above threshold [square root transformation = $f_2^{0.5}$-$f_1^{0.5}$ where f_2 and f_1 are the high and low limits of the receptive field 20 dB above threshold (Calford et al. 1983); Q_{10} = CF/bandwidth 10 dB above threshold (Kiang 1965)]. These numbers indicate remarkable breadth of tuning, and yet our estimates may underestimate maximum breadth of tuning at higher intensities since our stimulus set only spanned five octaves. Indeed, LFP receptive fields extended five octaves *below* CF at some high-frequency sites (CF 40 kHz). These bandwidths are much broader than estimates of bandwidth in primary ACx that are based on spike activity [e.g., average square root score of 0.39 $kHz^{0.5}$ (Calford et al. 1983) and 1.0 $kHz^{0.5}$ (Eggermont 1996); Q_{10} values average ~6-7 for CF of 8-12 kHz (Phillips and Irvine 1981)], and undoubtedly indicate that substantial portions of receptive fields are subthreshold. Simultaneous recordings of LFPs and spike activity explicitly demonstrate that LFP-based bandwidths are broader than spike-based bandwidths (Galvan 2001; Norena and Eggermont 2002), and prior intracellular studies have shown that subthreshold receptive fields extend beyond the boundaries of suprathreshold receptive fields (Ojima and Murakami 2002; Ribaupierre et al. 1972; Volkov and Galazjuk 1991; Wehr and Zador 2003).

The remarkable breadth of intracellular and LFP receptive fields raises the intriguing possibility that some primary ACx neurons may integrate information across much of the animal's audible spectrum. A recent study of gerbil primary ACx reached a similar conclusion based on the enhancement of multiunit responses by stimuli several octaves above the conventionally-defined receptive field (Schulze and Langner 1999). Other LFP(Eggermont 1996; Galvan et al. 2001; Norena and Eggermont 2002), multiple unit (Phillips and Hall 1992;

Phillips et al. 1994) and optical imaging (Bakin et al. 1996; Hess and Scheich 1996; Horikawa et al. 1996) studies also provide evidence for very broad spectral integration in primary ACx.

A potential cortical mechanism of acoustic processing

Since spike-based receptive fields have bandwidths that are similarly narrow throughout the lemniscal auditory system (Calford et al. 1983; Edeline et al. 1999), it is worth considering whether the broad, subthreshold receptive fields observed in the present study distinguish primary ACx from subcortical auditory nuclei (for now, we do not consider the nonlemniscal auditory regions within which broad receptive fields are, of course, more common (Calford and Webster 1981; Calford et al. 1983; Edeline et al. 1999), nor do we consider how inhibitory subfields are created (Sutter and Loftus 2003)). If, for example, neurons in all auditory nuclei have broad subthreshold receptive fields and narrow suprathreshold receptive fields, then the results of the present study do not reflect a unique feature of ACx. Alternatively, if subcortical nuclei have subthreshold receptive fields that are nearly as narrow as their suprathreshold receptive fields, then the breadth of cortical subthreshold receptive fields may indicate a unique cortical function.

There is evidence that subthreshold receptive fields in subcortical nuclei are narrower than those in cortex. For example, local application of the $GABA_A$ receptor antagonist bicuculline produces substantial expansion of receptive fields in primary ACx (Foeller et al. 2001; Muller and Scheich 1988; Wang et al. 2000; Wang et al. 2002), but reportedly lesser or no expansion in subcortical regions (Caspary et al. 1994; LeBeau et al. 2001; Palombi and Caspary 1992). The distinction between cortical and subcortical receptive fields applies to other sensory modalities, as well. In the somatosensory and visual systems, bicuculline similarly expands cortical, but not

thalamic, receptive fields (Dykes et al. 1984; Hicks et al. 1986; Sillito 1975), and intracellular recordings have demonstrated substantial subthreshold ("nonclassical" or "surround") receptive fields in cortex (Bringuier et al. 1999; Li and Waters 1996; Smits et al. 1991). Intracortical projections are thought to relay information for subthreshold receptive fields in somatosensory and visual cortex (Fox et al. 2003; Gilbert 1998), as is being proposed in the present study for primary ACx. These data suggest that subthreshold receptive fields are broader in each primary sensory cortex than in corresponding subcortical relays (although intracellular recordings in thalamic relay neurons will be needed to resolve this question fully).

Thus, broad subthreshold receptive fields may distinguish ACx from subcortical relays within the lemniscal pathway, and exist because they are created by intracortical circuitry (Hypothesis 3, above; Fig. 5B). If intracortical circuitry mediates integration across frequency representations, e.g., to generate responses to spectrally complex stimuli (Schulze et al. 1997; Whitfield and Evans 1965), then conventional spike-based receptive fields might actually reflect responses to suboptimal stimuli, i.e., pure tones. The present results predict one kind of optimal stimulus. The changes in onset latency with increasing spectral distance from CF ranged from ~1-4 ms/octave, depending on stimulus intensity. One prediction is that responses to multiple stimuli of different frequencies would sum optimally if their onsets coincided, i.e., if the stimuli were staggered in time with nonCF stimuli appearing before CF stimuli. The optimal stimulus may therefore be a sequence of stimuli—or, in the limit, a frequency-modulated (FM) sweep—moving toward CF from either higher or lower nonCFs, as shown previously (Heil et al. 1992; Phillips et al. 1985a). Complex stimuli such as FM sweeps are important features of natural sounds, including speech, to which ACx neurons respond (Fitch et al. 1997; Nelken et al. 1999; Steinschneider et al. 1999). Conversely, the inability to discriminate spectrally complex stimuli

following ACx lesions may underlie deficits in auditory perception such as "pure word deafness" in humans (Phillips 1998b).

Acknowledgements

We thank Dr. L. Kitzes and H. Rose for helpful comments on previous drafts of this manuscript. This study was supported by the NIDCD (DC-02967), NIDA (DA-12929), and by the California Tobacco–Related Disease Research Program (8RT-0059).

References

Bakin JS, Kwon MC, Masino SA, Weinberger NM, and Frostig RD. Suprathreshold auditory cortex activation visualized by intrinsic signal optical imaging. *Cereb Cortex* 6: 120-130, 1996.

Barth DS and Di S. Three-dimensional analysis of auditory-evoked potentials in rat neocortex. *J Neurophysiol* 64: 1527-1536, 1990.

Blanton MG, LoTurco JJ, and Kriegstein AR. Whole cell recording from neurons in slices of reptilian and mammalian cerebral cortex. *J Neurosci Meth* 30: 203-210, 1989.

Bringuier V, Chavane F, Glaeser L, and Fregnac Y. Horizontal propagation of visual activity in the synaptic integration field of area 17 neurons. *Science* 283: 695-699, 1999.

Brugge JF, Dubrovsky NA, Aitkin LM, and Anderson DJ. Sensitivity of single neurons in auditory cortex of cat to binaural tonal stimulation; effects of varying interaural time and intensity. *J Neurophysiol* 32: 1005-1024, 1969.

Calford MB and Webster WR. Auditory representation within principal division of cat medial geniculate body: an electrophysiological study. *J Neurophysiol* 45: 1013-1028, 1981.

Calford MB, Webster WR, and Semple MM. Measurement of frequency selectivity of single neurons in the central auditory pathway. *Hearing Res* 11: 395-401, 1983.

Caspary DM, Backoff PM, Finlayson PG, and Palombi PS. Inhibitory inputs modulate discharge rate within frequency receptive fields of anteroventral cochlear nucleus neurons. *J Neurophysiol* 72: 2124-2133, 1994.

Cruikshank SJ, Rose HJ, and Metherate R. Auditory thalamocortical synaptic transmission, in vitro. *J Neurophysiol* 87: 361-384, 2002.

Doron NN, Ledoux JE, and Semple MN. Redefining the tonotopic core of rat auditory cortex: physiological evidence for a posterior field. *J Comp Neurol* 453: 345-360, 2002.

Dykes RW, Landry P, Metherate R, and Hicks TP. Functional role for GABA in primary somatosensory cortex: shaping receptive fields of cortical neurons. *J Neurophysiol* 52: 1066-1093, 1984.

Edeline J-M, Hars B, Cotillon N, and Hennevin E. Muscimol diffusion after intracerebral microinjections: A re-evaluation based on electrophysiological and autoradiographic quantifications. *Neurobiol Learn Mem* 78: 100-124, 2002.

Edeline JM, Dutrieux G, Manunta Y, and Hennevin E. Diversity of receptive field changes in auditory cortex during natural sleep. *Eur J Neurosci* 14: 1865-1880, 2001.

Edeline JM, Manunta Y, Nodal FR, and Bajo VM. Do auditory responses recorded from awake animals reflect the anatomical parcellation of the auditory thalamus? *Hear Res* 131: 135-152, 1999.

Eggermont JJ. How homogeneous is cat primary auditory cortex? Evidence from simultaneous single-unit recordings. *Auditory Neurosci* 2: 79-96, 1996.

Eggermont JJ and Smith GM. Synchrony between single-unit activity and local field potentials in relation to periodicity coding in primary auditory cortex. *J Neurophysiol* 73: 227-245, 1995.

Evans EF. The frequency response and other properties of single fibres in the guinea-pig cochlear nerve. *J Physiol* 226: 263-287, 1972.

Fitch RH, Miller S, and Tallal P. Neurobiology of speech perception. *Annu Rev Neurosci* 20: 331-353, 1997.

Foeller E, Vater M, and Kossl M. Laminar analysis of inhibition in the gerbil primary auditory cortex. *J Assoc Res Otolaryngol* 2: 279-296, 2001.

Fox K, Wright N, Wallace H, and Glazewski S. The origin of cortical surround receptive fields studied in the barrel cortex. *J Neurosci* 23: 8380-8391, 2003.

Galvan VV. Long-term stability of frequency tuning and consolidation of learning-induced receptive field plasticity in the primary auditory cortex. *PhD Dissertation, University of California, Irvine*, 2001.

Galvan VV, Chen J, and Weinberger NM. Long-term frequency tuning of local field potentials in the auditory cortex of the waking guinea pig. *J Assoc Res Otolaryngol* 2: 199-215., 2001.

Gilbert CD. Adult cortical dynamics. *Physiol Rev* 78: 467-485, 1998.

Heil P and Irvine DRF. First-spike timing of auditory-nerve fibers and comparison with auditory cortex. *J Neurophysiol* 78: 2438-2454, 1997.

Heil P, Langner G, and Scheich H. Processing of frequency-modulated stimuli in the chick auditory cortex analogue: evidence for topographic representations and possible mechanisms of rate and directional sensitivity. *J Comp Physiol [A]* 171: 583-600, 1992.

Hess A and Scheich H. Optical and FDG mapping of frequency-specific activity in auditory cortex. *NeuroReport* 7: 2643-2647, 1996.

Hicks TP, Metherate R, Landry P, and Dykes RW. Bicuculline-induced alterations of response properties in functionally identified ventroposterior thalamic neurones. *Exp Brain Res* 63: 248-264, 1986.

Hind JE, Goldberg JM, Greenwood DG, and Rose JE. Some discharge characteristics of single neurons in the inferior colliculus of the cat. II. Timing of the discharges and observations on binaural stimulation. *J Neurophysiol* 26: 321-341, 1963.

Horikawa J, Hosokawa Y, Kubota M, Nasu M, and Taniguchi I. Optical imaging of spatiotemporal patterns of glutamatergic excitation and GABAergic inhibition in the guinea-pig auditory cortex in vivo. *J Physiol (Lond)* 497: 629-638, 1996.

Horikawa J, Ito S, Hosokawa Y, Homma T, and Murata K. Tonotopic representation in the rat auditory cortex. *Proc Japan Acad Ser B* 64: 260-263, 1988.

Hsieh CY, Cruikshank SJ, and Metherate R. Differential modulation of auditory thalamocortical and intracortical synaptic transmission by cholinergic agonist. *Brain Res* 880: 51-64, 2000.

Imig TJ and Morel A. Topographic and cytoarchitectonic organization of thalamic neurons related to their targets in low-, middle-, and high-frequency representations in cat auditory cortex. *J Comp Neurol* 227: 511-539, 1984.

Johnston D and Wu SM-S. *Foundations of cellular neurophysiology*. Cambridge, Mass.: MIT Press, 1995.

Kiang NY-S. *Discharge patterns of single fibers in the cat's auditory nerve*. Cambridge, Mass.,: M.I.T. Press, 1965.

Kilgard MP and Merzenich MM. Cortical map reorganization enabled by nucleus basalis activity. *Science* 279: 1714-1718, 1998.

Kitzes LM, Gibson MM, Rose JE, and Hind JE. Initial discharge latency and threshold considerations for some neurons in cochlear nuclear complex of the cat. *J Neurophysiol* 41: 1165-1182, 1978.

Langner G, Schreiner C, and Merzenich MM. Covariation of latency and temporal resolution in the inferior colliculus of the cat. *Hear Res* 31: 197-201, 1987.

LeBeau FE, Malmierca MS, and Rees A. Iontophoresis in vivo demonstrates a key role for GABA(A) and glycinergic inhibition in shaping frequency response areas in the inferior colliculus of guinea pig. *J Neurosci* 21: 7303-7312, 2001.

Li CX and Waters RS. In vivo intracellular recording and labeling of neurons in the forepaw barrel subfield (FBS) of rat somatosensory cortex: possible physiological and morphological substrates for reorganization. *Neuroreport* 7: 2261-2272, 1996.

Martin JH and Ghez C. Pharmacological inactivation in the analysis of the central control of movement. *J Neurosci Methods* 86: 145-159, 1999.

Mendelson JR, Schreiner CE, and Sutter ML. Functional topography of cat primary auditory cortex: response latencies. *J Comp Physiol [A]* 181: 615-633, 1997.

Merzenich MM, Knight PL, and Roth GL. Representation of cochlea within primary auditory cortex in the cat. *J Neurophysiol* 38: 231-249, 1975.

Metherate R and Aramakis VB. Intrinsic electrophysiology of neurons in thalamorecipient layers of developing rat auditory cortex. *Dev Brain Res* 115: 131-144, 1999.

Metherate R and Ashe JH. Facilitation of an NMDA receptor-mediated EPSP by paired-pulse stimulation in rat neocortex via depression of GABAergic IPSPs. *J Physiol (Lond)* 481: 331-348, 1994.

Metherate R and Ashe JH. Ionic flux contributions to neocortical slow waves and nucleus basalis-mediated activation: whole-cell recordings in vivo. *J Neurosci* 13: 5312-5323, 1993a.

Metherate R and Ashe JH. Nucleus basalis stimulation facilitates thalamocortical synaptic transmission in rat auditory cortex. *Synapse* 14: 132-143, 1993b.

Metherate R, Cox CL, and Ashe JH. Cellular bases of neocortical activation: modulation of neural oscillations by the nucleus basalis and endogenous acetylcholine. *J Neurosci* 12: 4701-4711, 1992.

Metherate R and Cruikshank SJ. Thalamocortical inputs trigger a propagating envelope of gamma-band activity in auditory cortex, *in vitro*. *Exp Brain Res* 126: 160-174, 1999.

Miller LM, Escabi MA, Read HL, and Schreiner CE. Functional convergence of response properties in the auditory thalamocortical system. *Neuron* 32: 151-160., 2001.

Muller CM and Scheich H. Contribution of GABAergic inhibition to the response characteristics of auditory units in the avian forebrain. *J Neurophysiol* 59: 1673-1689, 1988.

Muller-Preuss P and Mitzdorf U. Functional anatomy of the inferior colliculus and the auditory cortex: current source density analyses of click-evoked potentials. *Hear Res* 16: 133-142, 1984.

Nelken I, Rotman Y, and Yosef OB. Responses of auditory cortex neurons to structural features of natural sounds. *Nature* 397: 154-157, 1999.

Norena A and Eggermont JJ. Comparison between local field potentials and unit cluster activity in primary auditory cortex and anterior auditory field in the cat. *Hear Res* 166: 202-213, 2002.

Oertel D. The role of timing in the brain stem auditory nuclei of vertebrates. *Annu Rev Physiol* 61: 497-519, 1999.

Ohl FW, Scheich H, and Freeman WJ. Topographic analysis of epidural pure-tone-evoked potentials in gerbil auditory cortex. *J Neurophysiol* 83: 3123-3132, 2000.

Ojima H and Murakami K. Intracellular characterization of suppressive responses in supragranular pyramidal neurons of cat primary auditory cortex in vivo. *Cereb Cortex* 12: 1079-1091, 2002.

Palombi PS and Caspary DM. GABAA receptor antagonist bicuculline alters response properties of posteroventral cochlear nucleus neurons. *J Neurophysiol* 67: 738-746, 1992.

Phillips DP. Factors shaping the response latencies of neurons in the cat's auditory cortex. *Behav Brain Res* 93: 33-41, 1998a.

Phillips DP. Sensory representations, the auditory cortex, and speech perception. *Sem Hearing* 19: 319-332, 1998b.

Phillips DP and Hall SE. Multiplicity of inputs in the afferent path to cat auditory cortex neurons revealed by tone-on-tone masking. *Cerebral Cortex* 2: 425-433, 1992.

Phillips DP and Irvine DR. Responses of single neurons in physiologically defined primary auditory cortex (AI) of the cat: frequency tuning and responses to intensity. *J Neurophysiol* 45: 48-58, 1981.

Phillips DP, Mendelson JR, Cynader MS, and Douglas RM. Responses of single neurones in cat auditory cortex to time-varying stimuli: frequency-modulated tones of narrow excursion. *Exp Brain Res* 58: 443-454, 1985a.

Phillips DP, Orman SS, Musicant AD, and Wilson GF. Neurons in the cat's primary auditory cortex distinguished by their responses to tones and wide-spectrum noise. *Hearing Res* 18: 73-86, 1985b.

Phillips DP, Semple MN, Calford MB, and Kitzes LM. Level-dependent representation of stimulus frequency in cat primary auditory cortex. *Exp Brain Res* 102: 210-226, 1994.

Recanzone GH, Schreiner CE, and Merzenich MM. Plasticity in the frequency representation of primary auditory cortex following discrimination training in adult owl monkeys. *J Neurosci* 13: 87-103, 1993.

Ribaupierre Fd, Goldstein MH, and Yeni-Komshian G. Intracellular study of the cat's primary auditory cortex. *Brain Res* 48: 185-204, 1972.

Robles L and Ruggero MA. Mechanics of the mammalian cochlea. *Physiol Rev* 81: 1305-1352., 2001.

Roger M and Arnault P. Anatomical study of the connections of the primary auditory area in the rat. *J Comp Neurol* 287: 339-356, 1989.

Romanski LM and LeDoux JE. Organization of rodent auditory cortex: anterograde transport of PHA-L from MGv to temporal neocortex. *Cereb Cortex* 3: 499-514, 1993.

Rose HJ, Kaur S, and Metherate R. Synaptic processing in auditory cortex: data from in vivo intracellular recordings and the auditory thalamocortical slice. *Abstr Assoc Res Otolaryngol* 26: 314, 2003.

Rose JE, Hind JE, Anderson DJ, and Brugge JF. Some effects of stimulus intensity on response of auditory nerve fibers in the squirrel monkey. *J Neurophysiol* 34: 685-699., 1971.

Sally SL and Kelly JB. Organization of auditory cortex in the albino rat: sound frequency. *J Neurophysiol* 59: 1627-1638, 1988.

Sanes DH and Constantine-Paton M. The sharpening of frequency tuning curves requires patterned activity during development in the mouse, Mus musculus. *J Neurosci* 5: 1152-1166., 1985.

Schulze H and Langner G. Auditory cortical responses to amplitude modulations with spectra above frequency receptive fields: evidence for wide spectral integration. *J Comp Physiol [A]* 185: 493-508, 1999.

Schulze H, Ohl FW, Heil P, and Scheich H. Field-specific responses in the auditory cortex of the unanaesthetized Mongolian gerbil to tones and slow frequency modulations. *J Comp Physiol [A]* 181: 573-589., 1997.

Shaw NA. The auditory evoked potential in the rat--a review. *Prog Neurobiol* 31: 19-45, 1988.

Sillito AM. The contribution of inhibitory mechanisms to the receptive field properties of neurones in the striate cortex of the cat. *J Physiol (Lond)* 250: 305-329, 1975.

Smits E, Gordon DC, Witte S, Rasmusson DD, and Zarzecki P. Synaptic potentials evoked by convergent somatosensory and corticocortical inputs in raccoon somatosensory cortex: substrates for plasticity. *J Neurophysiol* 66: 688-695, 1991.

Steinschneider M, Volkov IO, Noh MD, Garell PC, and Howard MA, 3rd. Temporal encoding of the voice onset time phonetic parameter by field potentials recorded directly from human auditory cortex. *J Neurophysiol* 82: 2346-2357, 1999.

Sutter ML and Loftus WC. Excitatory and inhibitory intensity tuning in auditory cortex: evidence for multiple inhibitory mechanisms. *J Neurophysiol* 90: 2629-2647, 2003.

Talwar SK, Musial PG, and Gerstein GL. Role of mammalian auditory cortex in the perception of elementary sound properties. *J Neurophysiol* 85: 2350-2358., 2001.

Trussell LO. Synaptic mechanisms for coding timing in auditory neurons. *Annu Rev Physiol* 61: 477-496, 1999.

Volkov IO and Galazjuk AV. Formation of spike response to sound tones in cat auditory cortex neurons: interaction of excitatory and inhibitory effects. *Neuroscience* 43: 307-321, 1991.

Wang J, Caspary D, and Salvi RJ. GABA-A antagonist causes dramatic expansion of tuning in primary auditory cortex. *Neuroreport* 11: 1137-1140., 2000.

Wang J, McFadden SL, Caspary D, and Salvi R. Gamma-aminobutyric acid circuits shape response properties of auditory cortex neurons. *Brain Res* 944: 219-231, 2002.

Wehr M and Zador AM. Balanced inhibition underlies tuning and sharpens spike timing in auditory cortex. *Nature* 426: 442-446, 2003.

Weinberger NM and Bakin JS. Learning-induced physiological memory in adult primary auditory cortex: receptive fields plasticity, model, and mechanisms. *Audiol Neurootol* 3: 145-167, 1998.

Whitfield IC and Evans EF. Responses of auditory cortical neurons to stimuli of changing frequency. *J Neurophysiol* 28: 655-672, 1965.

Winer JA, Sally SL, Larue DT, and Kelly JB. Origins of medial geniculate body projections to physiologically defined zones of rat primary auditory cortex. *Hear Res* 130: 42-61, 1999.

Figure Legends

Fig.1. Intracellular (whole-cell) and local field potential (LFP) recordings from the same cortical location show similar CF and breadth of tuning. A. Intracellular responses from a layer 3 neuron (top traces) and LFP responses from the same layer 3 location (bottom traces) had a CF of 10 kHz, as evident from responses to 20 dB stimuli. Responses to 70 dB stimuli demonstrated intracellular and LFP bandwidths ≥5 octaves. Tone onset is at the beginning of each trace, as indicated by schematic at lower left (10 ms on/off ramp). B. Scatterplot showing similar intracellular and LFP bandwidths at 10-60 dB above response threshold at CF (n = 1-5 neurons / extracellular sites at each intensity). Dotted line indicates maximum detectable bandwidth, 5 octaves. C. Paired intracellular and LFP bandwidths (mean ± SE, same data as in B) at 10 dB and 20 dB above CF threshold did not differ (paired t-test, n = 4-5, $p > 0.05$; EPSP bandwidth (BW)10 (in octaves) = 1.25 ± 0.75, LFP BW10 = 2.2 ± 0.58; EPSP BW20 = 2.75 ± 0.85, LFP BW20 = 2.75 ± 0.63). IC, intracellular.

Fig. 2. EPSP and LFP onset latencies increase with spectral "distance" from CF. A. Superimposed LFP (top) and intracellular (bottom) responses show increase in onset latency with increasing spectral distance from CF (same data as in Fig. 1A, 70 dB; the 5 kHz stimulus-evoked LFP response had an onset latency similar to that for 20 kHz, but the trace crossed other responses and was removed for clarity). B. Sample LFP response to illustrate features measured quantitatively (see Methods). C. Average intracellular onset latencies show trend towards longer onset latencies with increasing spectral distance from CF, despite increased variability associated with more spectrally-distant means (n = 3 to 8 neurons for each mean value). Only latencies at –1 octave were significantly longer than at CF (one-tailed paired t-test, n = 7-8, $p < 0.05$).

Fig. 3. Features of tone-evoked LFPs in layer 4 of mid- and high-frequency cortical sites separated by ~2 mm. A, B. Example responses from mid- and high-frequency sites in the same animal. Only partial response sets are shown to demonstrate relevant features; tone onset is at beginning of each 50 ms trace. Arrows in this and subsequent figures indicate threshold for CF stimulus-evoked response. C. Onset latency data averaged from mid- and high-frequency sites in 19 animals, separately for each stimulus intensity (10-60 dB, relative to minimum threshold at each site). D. Onset latency for CF stimulus-evoked response at high-frequency site was consistently less than at mid-frequency site (paired t-test with all intensities grouped, $n = 17$, $p < 0.001$). For (C) and (D), data points are averages (± SE) from ≥ 3 animals. ANOVAs for each intensity level in (C) revealed significant differences for 10 and 30-60 dB at the mid-frequency site ($p < 0.01$), and 10-60 dB at the high-frequency site ($p < 0.05$).

Fig. 4. "Boosted" responses elicited by below-CF stimuli at higher intensities. All data in A-C from the same animal; tone onset at start of traces. Isointensity responses boxed in (A) are superimposed in (B) with amplitudes normalized to facilitate comparison of onset latencies. D. Intracellular responses to 5 kHz (CF) and 1.25 kHz stimuli at 70dB showing a boosted response to 1.25 kHz stimulus but shorter latency response to CF stimulus. E. Peak amplitude plotted vs. spectral distance from CF, at different intensites. Data from 19 animals, each data point is average (± SE) from ≥3 animals. ANOVAs for each intensity level revealed no significant differences at the mid-frequency site, and significant differences at 10-60 dB at the high-frequency site ($p < 0.01$)

Fig. 5. Two alternative hypotheses of thalamocortical and intracortical connectivity that could give rise to broad frequency tuning and increasing onset latencies with spectral distance from CF. A. Thalamocortical arbors are extensive and relay both CF and nonCF information from the thalamus directly to the recording site. B. CF information arrives at the recording site via thalamocortical projections, while nonCF information is relayed by intracortical projections.

Fig. 6. Muscimol reduced CF stimulus-evoked response amplitude but did not affect threshold or onset latency consistently. A. Example of muscimol-induced reduction of response magnitude, with no change in threshold (20 dB) or onset latency at most intensities. B. Muscimol reduced average peak amplitude of CF stimulus-evoked responses but did not change response threshold (repeated measures ANOVA, $p < 0.001$; paired t-test vs. pre-drug at each intensity, n = 5-9 pairs, $p < 0.05$, except –10 dB, $p >> 0.05$). Control saline injections had little effect (paired t-test vs. pre-drug at each intensity, n = 5, $p > 0.05$). C. Muscimol did not alter average onset latency consistently (paired t-test vs. pre-drug at each intensity, n = 5-9 pairs, $p > 0.05$ with the exception of 40 dB, $p < 0.05$).

Fig. 7. Reduction of receptive field bandwidth by muscimol. A. Example of effect on tone-evoked responses at mid-frequency site. Intracortical microinjection of muscimol (5.1 mM, 1 µl) reduced response amplitude without affecting CF threshold. Note that responses to some nonCF stimuli appear to be reduced completely. B. Response amplitudes in muscimol expressed as a percent of pre-drug peak amplitude, for CF stimuli (n = 5-9 at each intensity) and nonCF stimuli (data from 1-3 octaves below CF combined for each experiment, n = 5-9 at each intensity except n = 1 for 10 dB; paired t-test comparing responses evoked by CF stimuli and nonCF stimuli, $p <$

0.05 at 20 dB). C. Muscimol reduced average bandwidth 20-50 dB above CF stimulus-evoked response threshold (paired t-test, n = 5-9 at each intensity, $p < 0.05$), but not 60-70 dB above threshold ($p > 0.05$). Dotted line indicates maximum detectable bandwidth, 5 octaves.

Fig 8. Picrotoxin reverses inihibition by muscimol. A. Schematic of experimental design showing picrotoxin diffusing from the electrode to act locally at the recording site, whereas muscimol, previously delivered by intracortical micoinjection, inhibits a much larger region of cortex. B. Example showing muscimol (200 μM, 3 μl) –induced reduction of responses to CF and nonCF (-3 octaves) stimuli, and reversal of inhibition by picrotoxin (100 nM in saline). Reversal of inhibition was greater for CF stimulus-evoked responses than for nonCF stimulus-evoked responses.

Fig. 9. Picrotoxin diffusing from the recording electrode preferentially disinhibits responses to CF stimuli over responses to nonCF stimuli (3 octaves below CF). A. Average data showing greater reversal by picrotoxin of muscimol-inhibited responses to CF stimuli (i) compared to responses to nonCF stimuli (ii) (repeated measures ANOVA, n = 6-8 for each intensity, $p < 0.001$ for CF and nonCF comparisons: pre-drug vs muscimol, muscimol vs picrotoxin, pre-drug vs picrotoxin). B. Average responses after muscimol and picrotoxin expressed as percentage of pre-drug values. Muscimol reduced response amplitude similarly for both CF and nonCF stimuli, but responses to CF stimuli show a greater recovery after picrotoxin (Factorial ANOVA comparing CF and nonCF 30–60 dB after picrotoxin, n = 6-8, $p < 0.001$). Note that the effect of picrotoxin on CF stimulus-evoked responses varied with intensity (regression analysis, R^2 =

0.124, $p < 0.05$; correlation of nonCF stimulus-evoked responses with intensity was not significant).

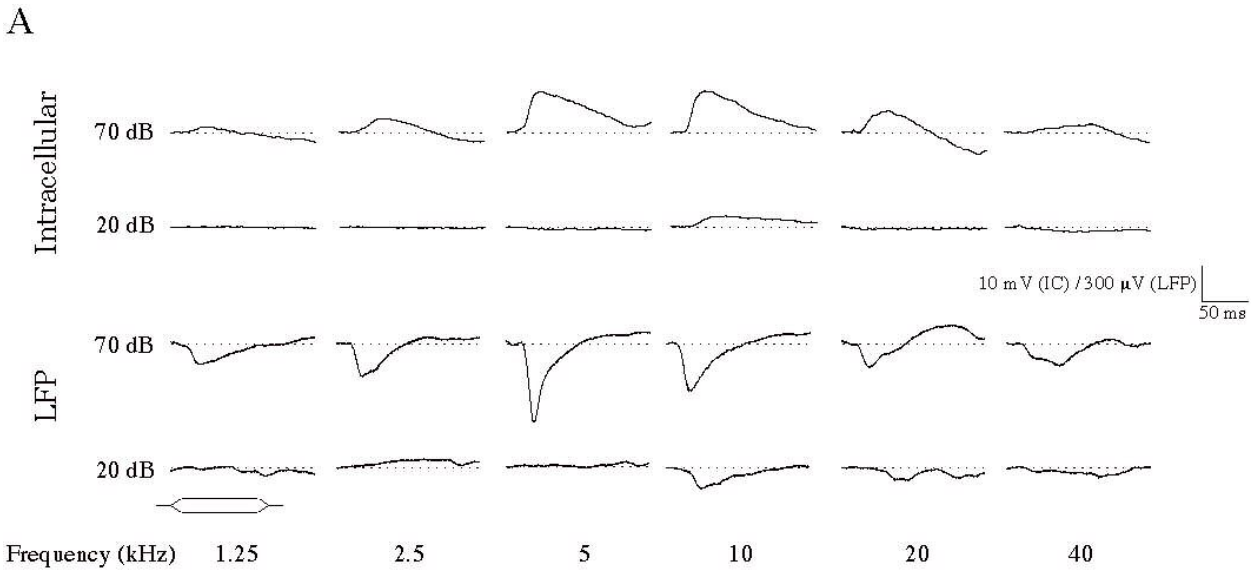
A
Intracellular
70 dB
20 dB
10 mV (IC) / 300 µV (LFP)
50 ms
LFP
70 dB
20 dB
Frequency (kHz) 1.25 2.5 5 10 20 40

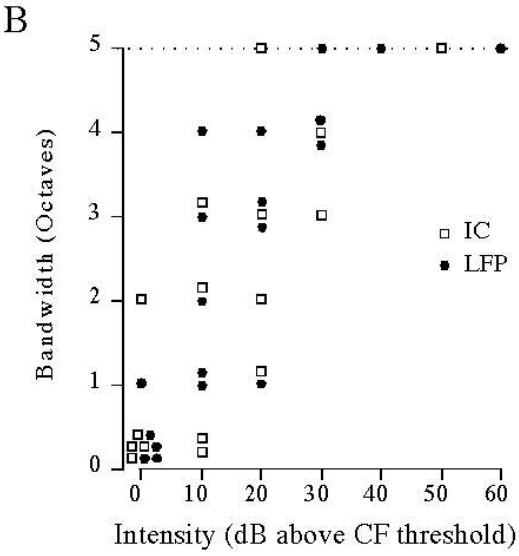
B
Bandwidth (Octaves)
IC
LFP
Intensity (dB above CF threshold)

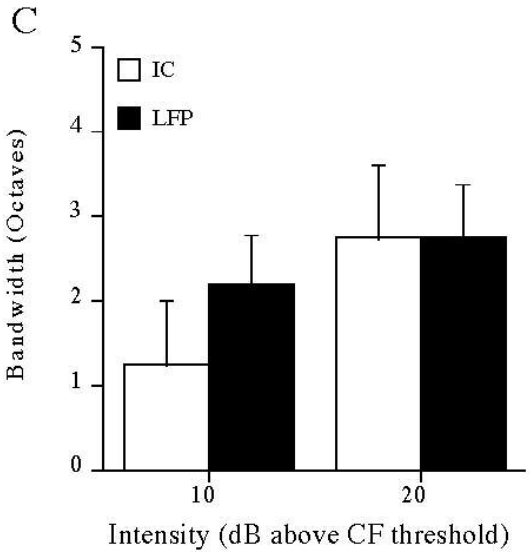
C
Bandwidth (Octaves)
IC
LFP
Intensity (dB above CF threshold)

Figure 1

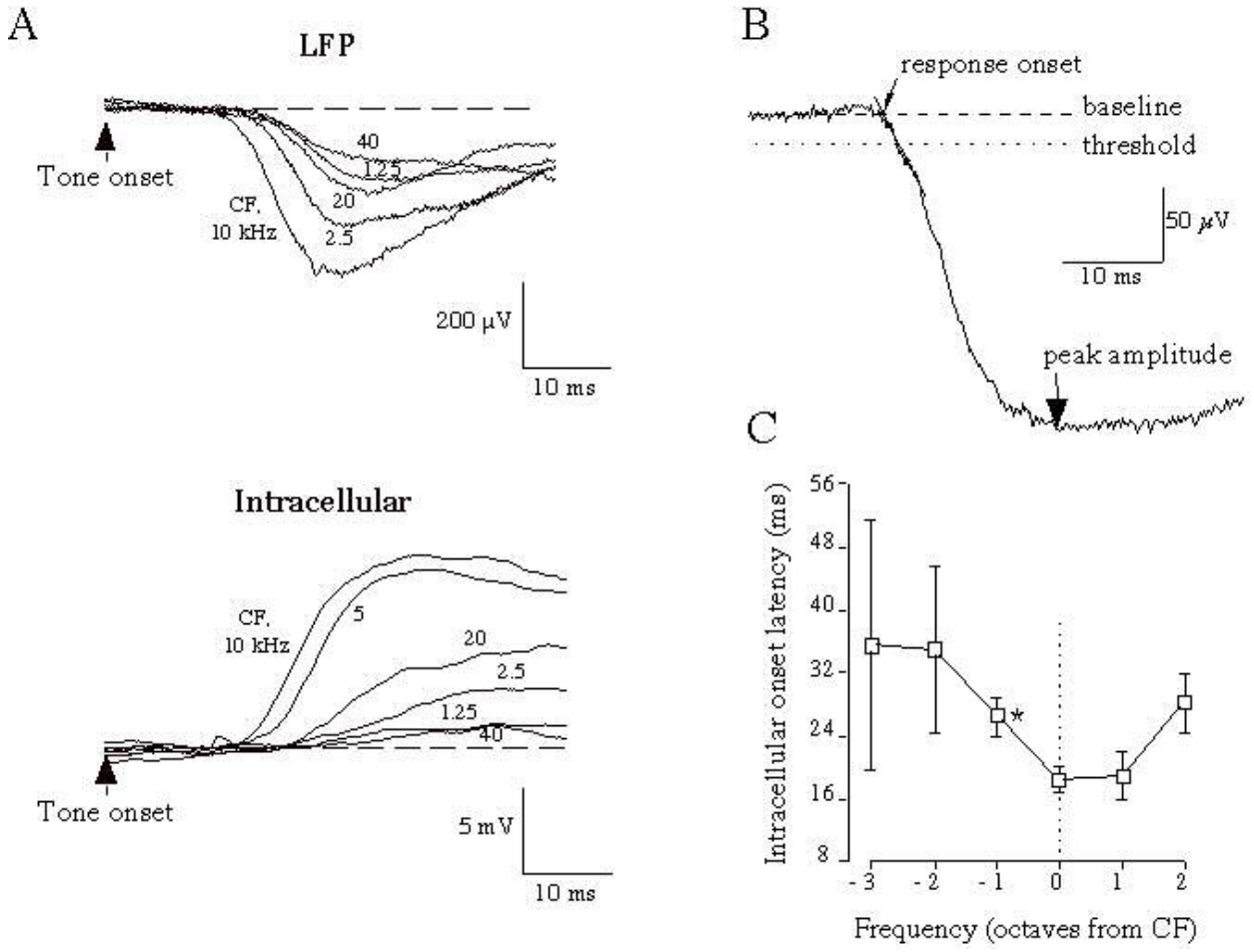
A
LFP
Tone onset
CF,
10 kHz
40
1.25
20
2.5
200 µV
10 ms
Intracellular
CF,
10 kHz
5
20
2.5
1.25
4.0
Tone onset
5 mV
10 ms
B
response onset
baseline
threshold
50 µV
10 ms
peak amplitude
C
Intracellular onset latency (ms)
56
48
40
32
24
16
8
-3
-2
-1
0
1
2
Frequency (octaves from CF)

Figure 2

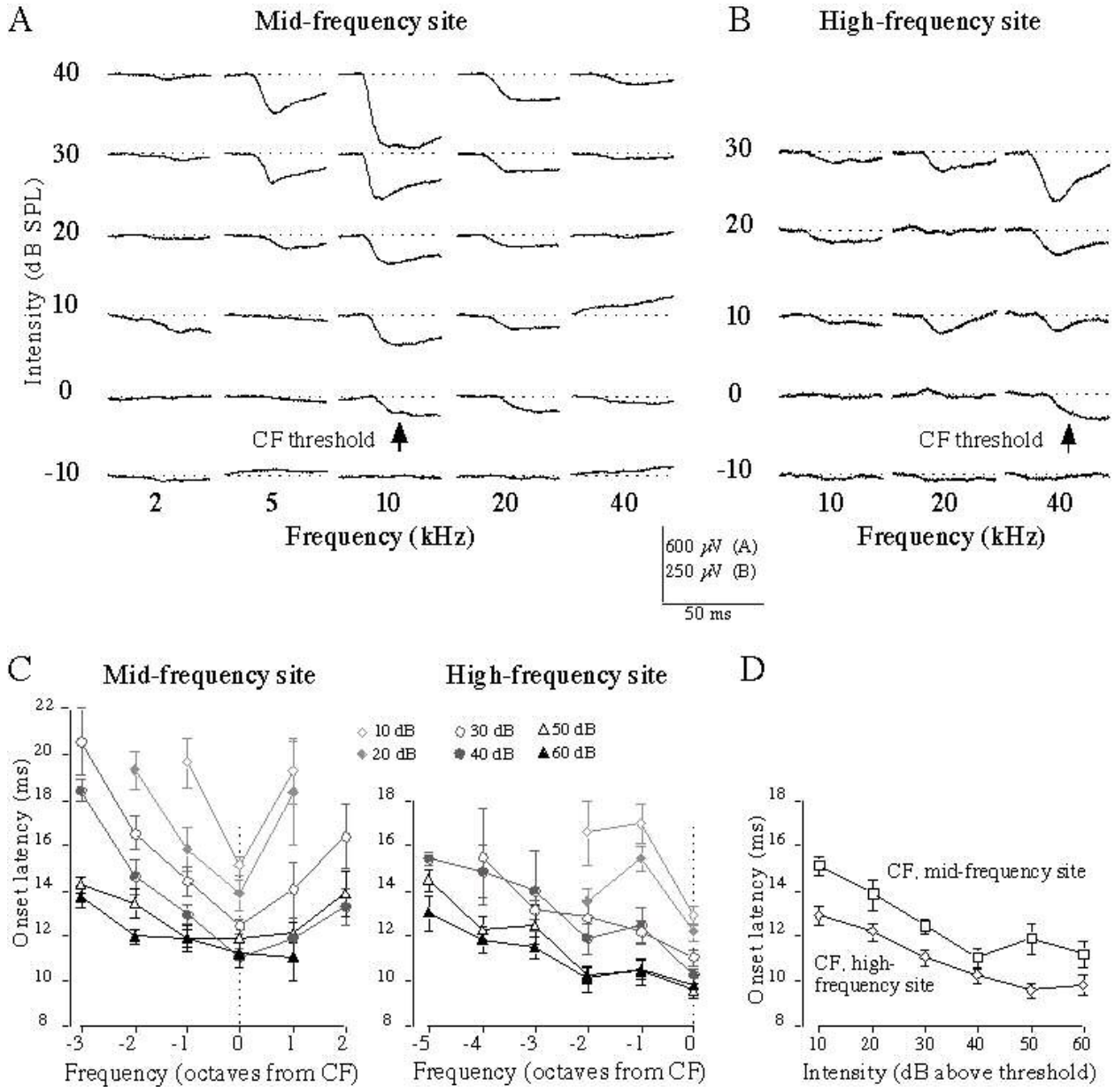
A
Mid-frequency site
B
High-frequency site
Intensity (dB SPL)
CF threshold
Frequency (kHz)
600 μV (A)
250 μV (B)
50 ms
C
Mid-frequency site
High-frequency site
10 dB
20 dB
30 dB
40 dB
50 dB
60 dB
Onset latency (ms)
Frequency (octaves from CF)
D
CF, mid-frequency site
CF, high-frequency site
Intensity (dB above threshold)

Figure 3

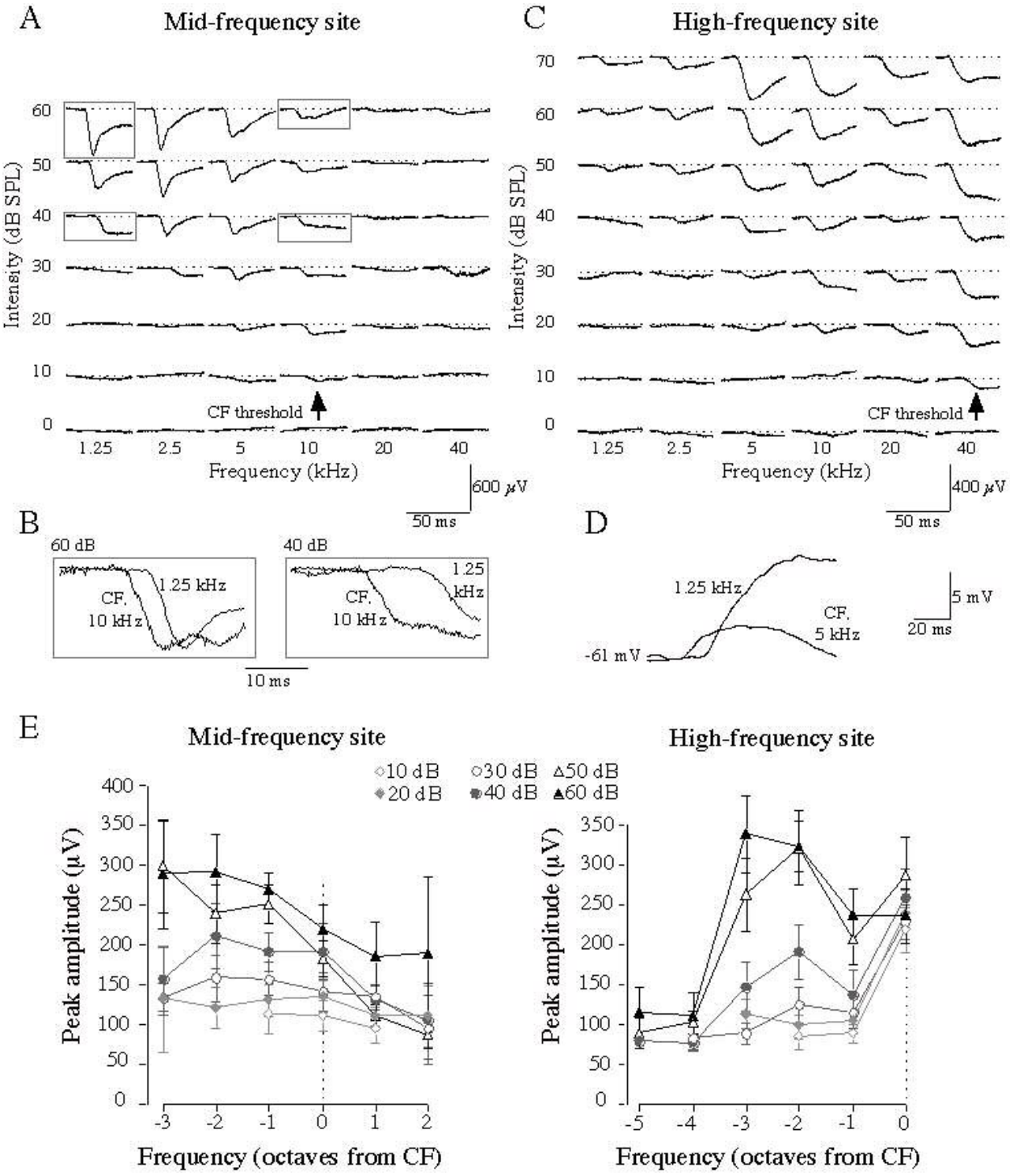
A
Mid-frequency site
Intensity (dB SPL)
60
50
40
30
20
10
0
CF threshold
1.25
2.5
5
10
20
40
Frequency (kHz)
600 μV
50 ms
C
High-frequency site
70
60
50
40
30
20
10
0
CF threshold
1.25
2.5
5
10
20
40
Frequency (kHz)
400 μV
50 ms
B
60 dB
CF, 10 kHz
1.25 kHz
40 dB
CF, 10 kHz
1.25 kHz
10 ms
D
1.25 kHz
CF, 5 kHz
-61 mV
5 mV
20 ms
E
Mid-frequency site
10 dB
20 dB
30 dB
40 dB
50 dB
60 dB
Peak amplitude (μV)
400
350
300
250
200
150
100
50
0
-3
-2
-1
0
1
2
Frequency (octaves from CF)
High-frequency site
Peak amplitude (μV)
350
300
250
200
150
100
50
0
-5
-4
-3
-2
-1
0
Frequency (octaves from CF)

Figure 4

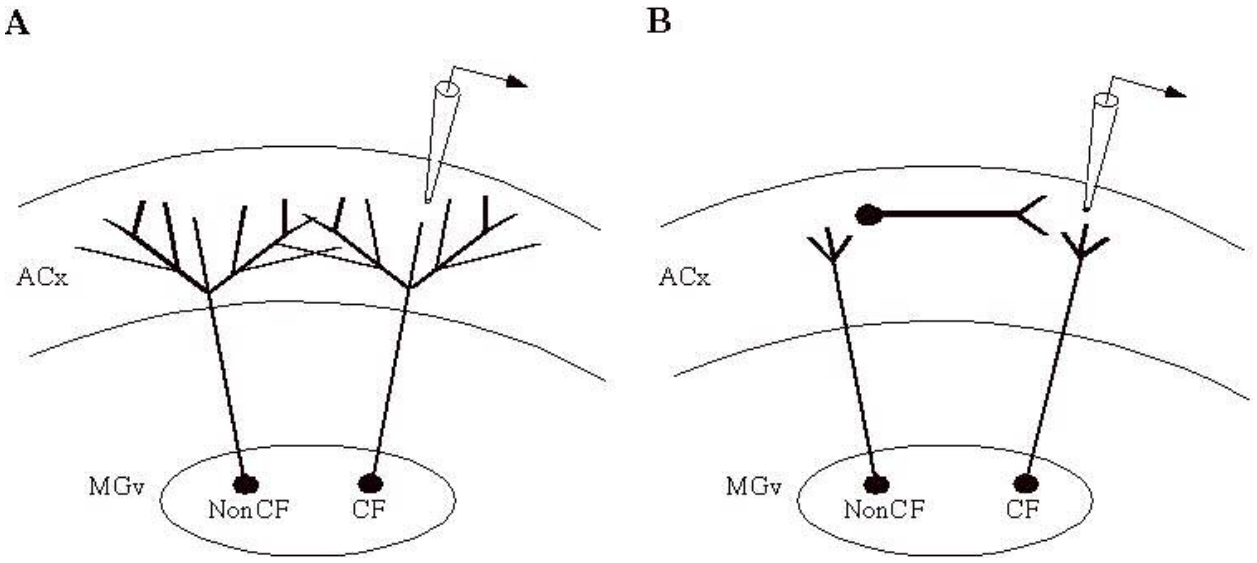

Figure 5

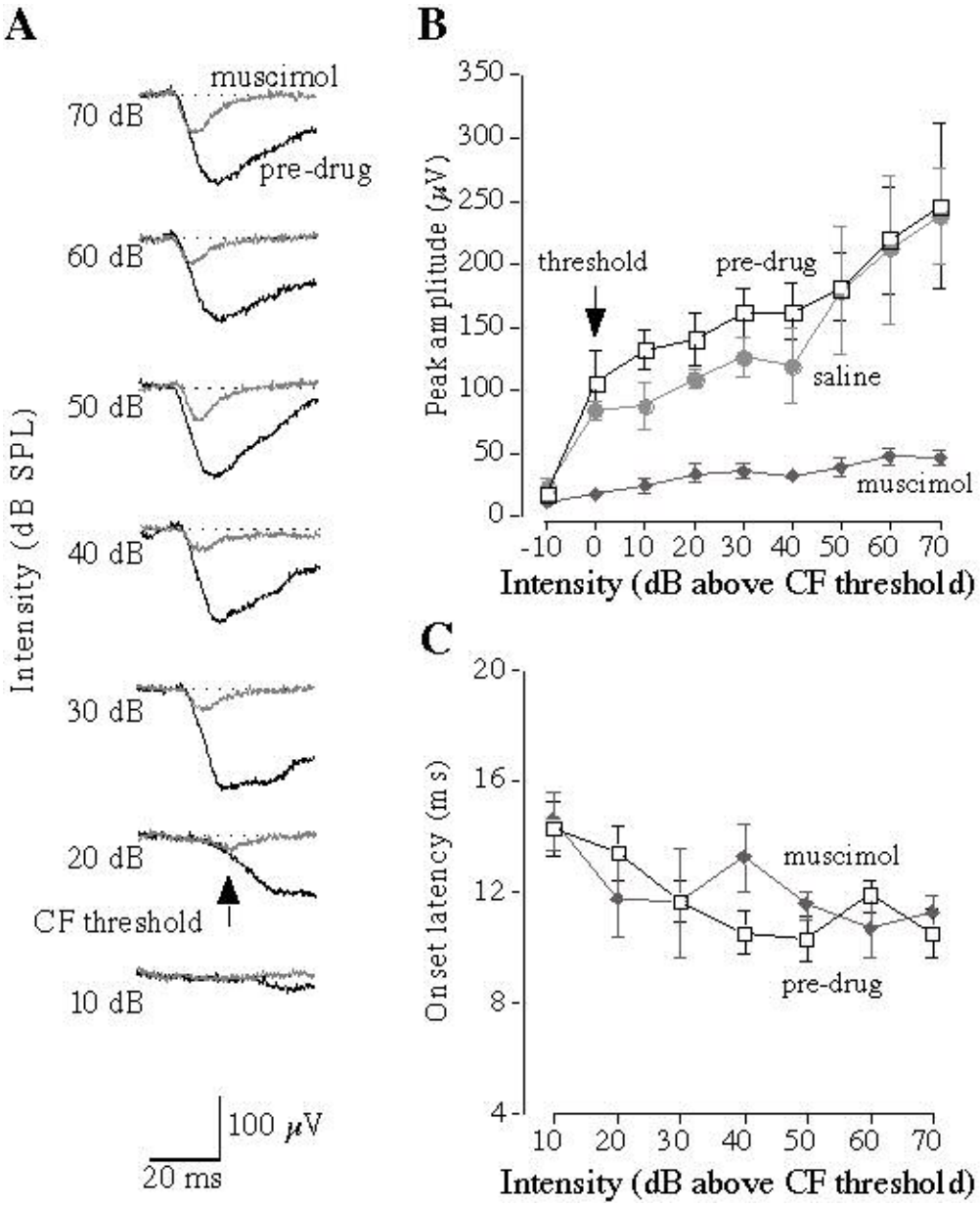
A
muscimol
70 dB
pre-drug
60 dB
50 dB
40 dB
30 dB
20 dB
CF threshold
10 dB
Intensity (dB SPL)
100 μV
20 ms
B
Peak amplitude (μV)
threshold
pre-drug
saline
muscimol
Intensity (dB above CF threshold)
C
Onset latency (ms)
muscimol
pre-drug
Intensity (dB above CF threshold)

Figure 6

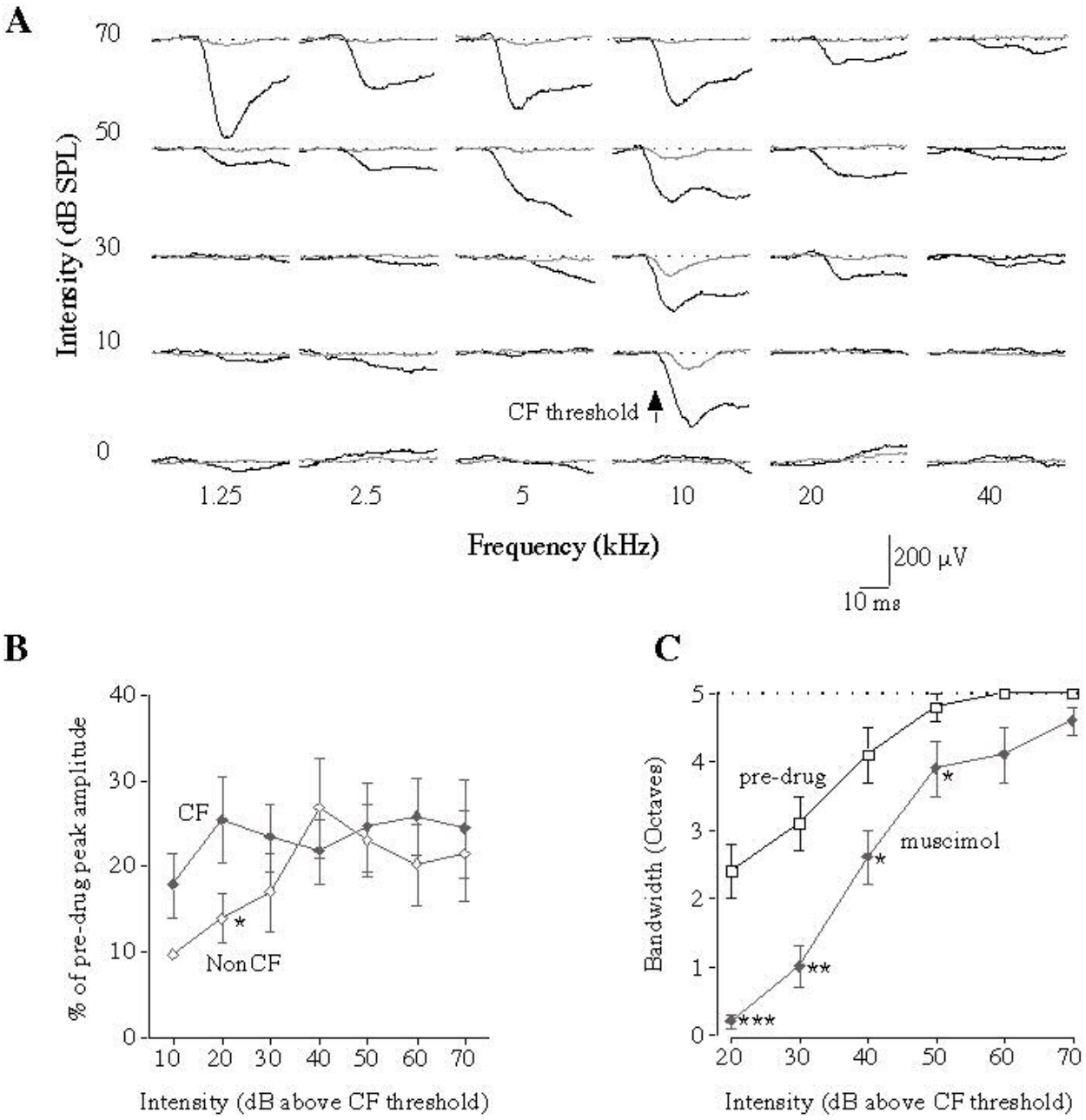
A
70
50
30
10
0
Intensity (dB SPL)
CF threshold
1.25
2.5
5
10
20
40
Frequency (kHz)
200 μV
10 ms
B
% of pre-drug peak amplitude
CF
Non CF
*
Intensity (dB above CF threshold)
C
Bandwidth (Octaves)
pre-drug
muscimol
*
**
***
Intensity (dB above CF threshold)

Figure 7

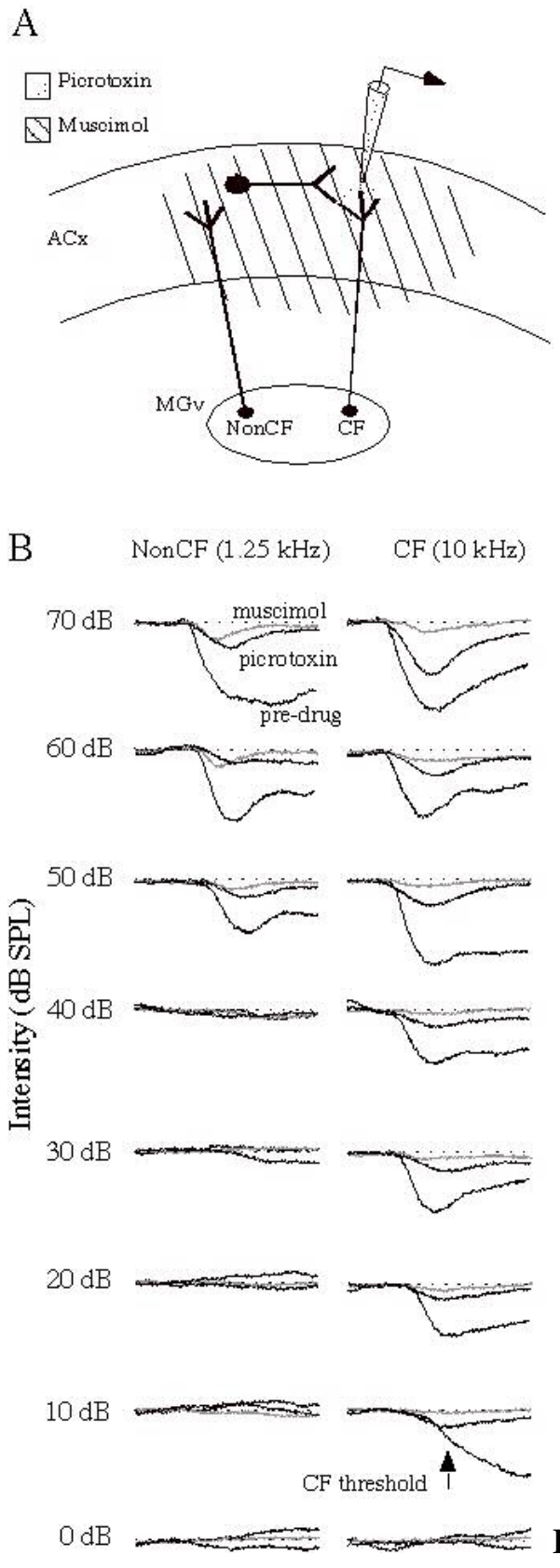
A
Picrotoxin
Muscimol
ACx
MGv
NonCF
CF
B
NonCF (1.25 kHz)
CF (10 kHz)
70 dB
muscimol
picrotoxin
pre-drug
60 dB
50 dB
40 dB
30 dB
20 dB
10 dB
CF threshold
0 dB
Intensity (dB SPL)

Figure 8

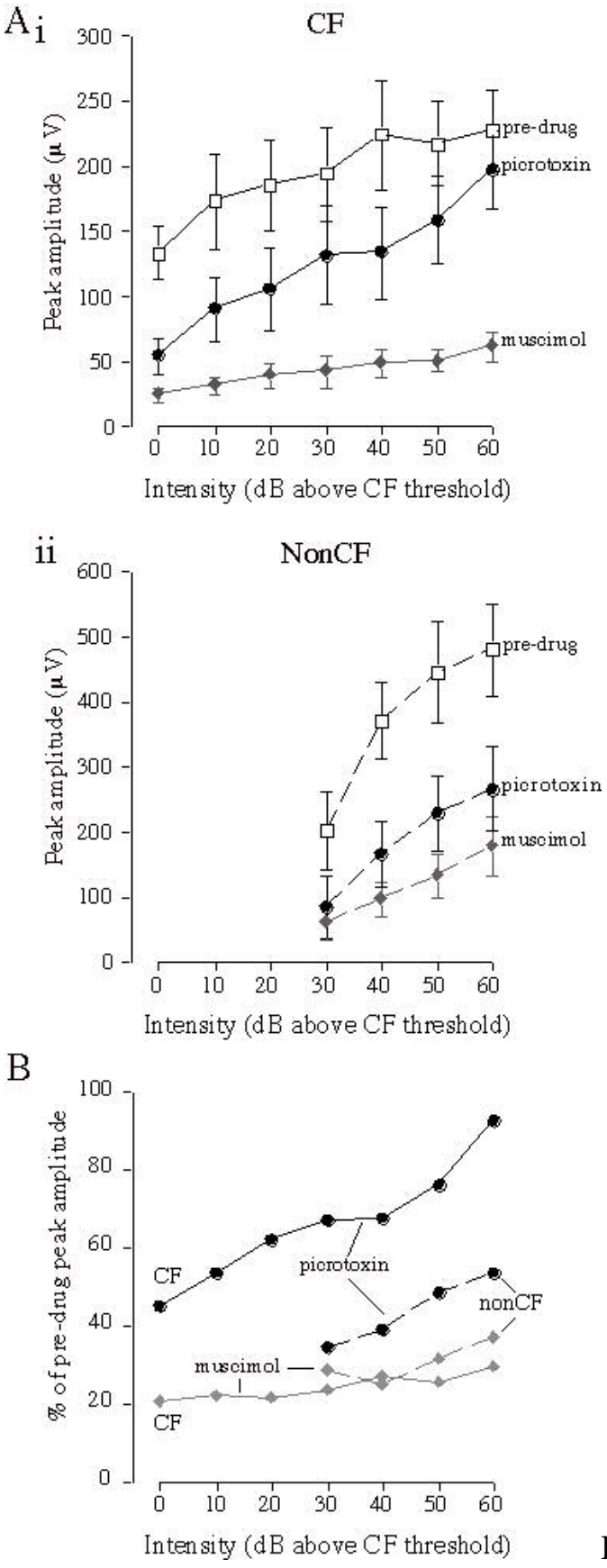
Ai
CF
Peak amplitude (μV)
pre-drug
picrotoxin
muscimol
Intensity (dB above CF threshold)
ii
NonCF
Peak amplitude (μV)
pre-drug
picrotoxin
muscimol
Intensity (dB above CF threshold)
B
% of pre-drug peak amplitude
CF
picrotoxin
nonCF
muscimol
CF
Intensity (dB above CF threshold)

Figure 9